P.D.
539.7
G326
V 2, No 2.

TECHNICAL PROGRESS REVIEWS

POWER REACTOR TECHNOLOGY

Prepared for U. S. ATOMIC ENERGY COMMISSION by GENERAL NUCLEAR ENGINEERING CORP.

ILLINOIS STATE LIBRARY
APR 3 - 1959
U. S. Sept. of Documents Deposit

MARCH 1959 VOLUME 2 NUMBER 2

TECHNICAL PROGRESS REVIEWS

To meet the needs of industry for concise summaries of current atomic developments, the AEC is publishing this series, Technical Progress Reviews. Issued quarterly, each of the reviews digests and evaluates the latest findings in a specific area of nuclear technology and science.

The three journals currently published in this series are:

Power Reactor Technology, Walter H. Zinn and associates, General Nuclear Engineering Corporation

Reactor Fuel Processing, Stephen Lawroski and associates, Chemical Engineering Division, Argonne National Laboratory

Reactor Core Materials (covering solid material developments), R. W. Dayton, E. M. Simons, and associates, Battelle Memorial Institute

Each journal may be purchased ($2.00 per year for subscription and individual issues $0.55) from the Superintendent of Documents, U. S. Government Printing Office, Washington 25, D. C. See back cover for remittance instructions and foreign postage requirements.

Availability of Reports Cited in This Review

Unclassified AEC reports are available for inspection at AEC depository libraries and are sold by the Office of Technical Services, Department of Commerce, Washington 25, D. C.

Unclassified reports issued by other Government agencies or private organizations should be requested from the originator.

Unclassified British and Canadian reports may be inspected at AEC depository libraries. British reports are sold by the British Information Service, 30 Rockefeller Plaza, New York, N. Y.; Canadian reports (AECL series) are sold by the Scientific Document Distribution Office, Atomic Energy of Canada, Ltd., Chalk River, Ontario, Canada.

Classified U. S. and foreign reports identified in this journal as Secret or Confidential may be purchased by properly cleared Access Permit Holders from the Technical Information Service Extension, U. S. Atomic Energy Commission, P. O. Box 1001, Oak Ridge, Tenn. Such reports may be inspected at classified AEC depository libraries.

PD
539.7
G326
V 2, N 2

POWER REACTOR TECHNOLOGY

a review of recent developments prepared by

GENERAL NUCLEAR ENGINEERING CORP.

MARCH 1959 VOLUME 2 NUMBER 2

foreword

This quarterly review of reactor development has been prepared at the request of the Division of Information Services of the United States Atomic Energy Commission. Its purpose is to assist interested organizations in the task of keeping abreast of new results in reactor technology for civilian application.

The report is a concise discussion of selected phases of research and development for which there have been significant advances or a heightened interest in the past few months. It is not meant to be a comprehensive abstract of all material published during the quarter nor is it meant to be a treatise on any part of the subject. The intention is to cover the various areas of reactor development from the general viewpoint of the reactor designer rather than from the more detailed points of view of specialists in the individual areas. However, papers which are thought to be of particular significance or of particular usefulness in specialized fields will be mentioned in short notes. In the over-all plan of the report, it is intended that various subjects will be treated from time to time and will be brought up to date at that time.

Any interpretation of results which is given represents only the opinion of the editors of the report, who are General Nuclear Engineering Corporation personnel. Readers are urged to consult the original references in order to obtain all of the background of the work reported and to obtain the interpretation of the results given by the original authors.

W. H. ZINN
General Nuclear Engineering Corporation

contents

ii		Foreword
1		**GENERAL RESEARCH AND DEVELOPMENT**
1	I	APPLICATIONS: NUCLEAR SHIP PROPULSION
1		General Economic Considerations
2		Current Construction Projects and Design Studies
4		American-Standard Study
6		Hazard Considerations
7	II	REACTOR PHYSICS
7		Reactor Physics Constants
7		Neutron Slowing Down
11		Physics of Low-enrichment and Light-water Reactors
13		Doppler Coefficient for U^{238}
14		Effect of Holes on Slowing Down and Diffusion Areas
16		Recent Measurements on DIMPLE and GLEEP
18		Estimated Reactivity Lifetime in D_2O Reactors
23	III	THERMAL CONSIDERATIONS
23		Heat Transfer and Thermal Cycles for Gas-cooled Systems
26		Properties of Gases
28	IV	REACTOR CONTROL: BURNABLE POISONS
30	V	SHIELDING
30		Neutron-flux Distribution and Attenuation
31		Concretes for Reactor Shielding
33	VI	FUEL ELEMENTS
33		Electron-beam Vacuum-welding Process
34		Electrocladding of Fuel Elements
34		Lead Bonding of Fuel Elements

contents (continued)

36 VII OTHER REACTOR MATERIALS

36 Graphite
38 Zirconium and Zirconium Alloys
40 Miscellaneous Components

42 VIII FUEL CYCLES

42 U^{236} Problem in Isotope Separation Plants
42 Isotope Build-up in Recycled Fuel

44 **PROGRESS ON SPECIFIC REACTOR TYPES**

44 IX HEAVY-WATER REACTORS: LEAKAGE DETECTION

45 Quantitative Analysis of Water Mixtures
45 Continuous-flow Heavy-water Analyses
46 Heavy-water Vapor Leakage Detection
46 Monitoring for Tritium in the Air
47 Monitoring for Tritium Contamination of Surfaces

49 X BOILING REACTORS: TURBINE CORROSION AND EROSION

Issued quarterly by the U. S. Atomic Energy Commission. Use of funds for printing this publication approved by the Director of the Bureau of the Budget on Nov. 1, 1957.

APPLICATIONS: NUCLEAR SHIP PROPULSION

General Economic Considerations

The success of nuclear submarines in the United States has demonstrated the technical feasibility of nuclear ship propulsion. The economic feasibility in commercial applications remains to be demonstrated. A number of reports, one covering a very extensive study,[1] have recently treated the subjects of nuclear ship propulsion and its economic relationships.

Many of the economic factors in ship propulsion are similar to those which govern the economics of central station nuclear power. Two new variables enter, however: (1) the weight of the nuclear plant per unit of output (which in comparative evaluations is balanced against the weight of a conventional propulsion plant plus that of its fuel requirement for a given voyage), and (2) the speed at which the ship is to be driven (which is determined by the capacity of the plant installed in the ship). In addition to these new considerations, the consideration of reactor safety enters the economic picture perhaps more strongly than in the case of the central station reactor because (1) the propulsion reactor is more subject to external hazards, such as collisions, and (2) because the hazard problems are international rather than national ones.

Aside from the foregoing considerations, the main economic characteristics, as in the case of the central station plant, can be grouped into those which affect capital cost and those which affect fuel cost. There is no doubt that the capital cost of a nuclear propulsion system will exceed that of a conventional system by a very substantial margin. With regard to capital cost the nuclear ship propulsion plant has, in one respect, a less favorable competitive situation than does the central station reactor, for there does not appear to be an immediate prospect for very high-power propulsion plants, and it is well established that the nuclear plant competes more favorably in the larger sizes. In another respect, however, its position is more favorable. Its cost represents only a fraction of the total investment in the ship, and therefore the economic effects of performance improvements, such as higher speed or higher use factor, which the nuclear plant may provide, are proportionately magnified.

In the area of fuel costs nuclear plants are potentially cheaper than conventional plants, and indeed, it may be said that unless this potentiality is realized there is little hope of competing successfully. The fuel oil used for marine fuel is considerably more expensive than the fuel used in the average central station plant. Reference 1 quotes a value of $3.00 per barrel as an average price at the docks in the United States; this corresponds to about 50 cents per billion British thermal units or 2 mills per thermal kilowatt hour. However, the attainment of low fuel cost will be more difficult in propulsion reactors than in central station reactors because of the high neutron loss by leakage which tends to characterize the relatively small propulsion reactors. Further difficulties may arise in specific cases because of the very great emphasis on reactor safety. For example, this emphasis may dictate the use of steel rather than zirconium for fuel jackets in water-cooled reactors.

Because of the performance variables of ship speed and specific weight of the propulsion plant, as well as the variety of ship applications, there exists a wide range of possible circumstances under which nuclear propulsion might be considered, and there is reason to expect that nuclear propulsion will be competitive in specific applications long before it becomes generally competitive.

Current ship designs and design speeds have evolved from the economic relations peculiar to their fossil-fueled propulsion plants. It would be expected that the application of nuclear power would lead to changes in these characteristics which would improve the competitive position of the nuclear plant over that which would apply if a nuclear plant were simply substituted for a conventional plant in a specific ship. In particular, it would be expected that the speeds of nuclear ships would be higher, since the main restrictions on speed in conventional ships are the cost and the weight and space requirements of fuel oil. However, the speed-resistance relationship for surface ships will probably limit the speed increase to a modest one. For a given ship, the required propulsion power increases with speed (V) at a rate higher than the third power of V. Consequently, in current studies of nuclear propulsion for nonpassenger ships, one does not find postulated speeds higher than about 25 knots. For completely submerged vessels the power requirement increases about V^3; hence, for such types, higher speeds might be considered. Reference 2, which treats a submarine tanker of 30,000 deadweight ton cargo capacity and a cruising speed of 22 knots, finds that at speeds less than about 19 knots the submarine power requirements are higher than those of a surface tanker of equal capacity, but at higher speeds the surface propulsion requirements become much higher. For example, at the crossover point of 19 knots the required power is about 26,000 SHP, whereas at 20 knots the surface propulsion requirement has increased to about 43,000 SHP as against about 29,000 SHP for the submarine.

With regard to ship size it might be expected that very large ships would give a large improvement in the competitive position of nuclear propulsion, since the specific capital cost (dollars per installed shaft horsepower) of nuclear plants tends to decrease rather rapidly with plant output. However, for a given surface speed the propulsion power requirement increases rather slowly with ship displacement, and it is probably only when larger displacement can be accompanied by a substantial speed increase (by a factor of 2 or more) that an important gain can be made. Actually, reference 1 concludes that nuclear propulsion is particularly attractive in trades that require small ships on long trade routes (see the following section).

Current Construction Projects and Design Studies

There are currently two nonmilitary nuclear vessels under construction, the N. S. Savannah[3] in the United States and the icebreaker Lenin[4] in the USSR. Of these, the Lenin is obviously not a cargo vessel. The Savannah, designed for passenger-cargo service, may be compared with other vessels of this type with respect to costs. The major characteristics of the reactors for these two vessels are listed in Table I-1 along with reactor characteristics from a number of ship propulsion design studies.

It has been stated[3] that an objective of the Savannah program is to gain general world acceptance of nuclear ships in commerce, and consequently the Savannah design includes a high standard of safety and reliability. That the design is conservative with respect to factors which affect power density, coolant circulation rate, and system weight is evident by comparison with the icebreaker characteristics in Table I-1.

The Savannah is scheduled for delivery[3] in 1960. The ship is a single screw combination passenger-cargo vessel, 595½ ft long, with a 78-ft beam, a 29½-ft draft, and a 21,800-ton displacement. It will accommodate 60 to 100 passengers and carry 10,000 tons of cargo. The designed normal speed is 20 knots.[5]

The ship is to be powered by a 74 Mw(t) pressurized water reactor with two main coolant loops and steam generators which will produce 22,000 SHP at the propeller. The reactor vessel will consist of a 26-ft cylindrical shell 98 in. in inside diameter, with a hemispherical head at the bottom and a dished head on top. The nuclear plant, including the containment and shielding, is located amidship. The ship's conventional propulsion turbines will utilize saturated steam. Emergency power for ships service, reactor cooling, and take-home power will be furnished by two 750-kw diesel generators and two auxiliary boilers which bring take-home power to 3,000 SHP.

The primary system is contained in a cylindrical steel vessel, 35 ft in diameter by 51 ft long and 2½ in. thick, lying fore and aft along the centerline of the ship. The vessel is designed to resist the maximum pressure (186 psi) that could result from the flashing of all the primary water to steam.

Table I-1 COMPARISON OF MARINE REACTORS

Application	N. S. Savannah[3] (USA)	Lenin[4] (USSR)	Design study[5] (USA)	Design study[7] (UK)	Design study[7] (UK)	Design study[8] (France)	Design study[8] (France)	Design study[8] (France)	Design study[6] (Japan)
Type	PWR	PWR	OMR	GCR	GCR	PWR	BWR	GCR	PWR
Number installed	1	3							
Core data									
Diameter, ft	5.1	~3	6	14	4.75	4.8	5.1	11.5	5.2
Height, ft	5.5	~4.8	6.8	13	4.75	4.5	5.1	11.5	4.8
Fuel	Sint. UO_2 pellets	Sintered UO_2	U metal	U metal	U–S.S. cermet	UO_2	UO_2 pellets	Sintered UO_2	UO_2 pellets
Enrichment, %	4	5	1.6	Several	~15	1.5	1.5	1.8	1.7
Cladding	S.S.	Zr alloy	Al	Mg alloy		Zr or S.S.	Zr	S.S.	Zr
U^{235} inventory, kg	330	85	352			~100	~120	117	140
Moderator	H_2O	H_2O	Terphenyl	Graphite	Graphite	H_2O	H_2O	Graphite	H_2O
Thermal data									
Mw(t)	74 (max.)	90 (nom.)	100	~150*	~150*	~50	51	60	100
Heat flux, Btu/(hr)(ft)(sq)	57,100 (avg.)	369,000 (max.)	33,800 (avg.)						132,000 (avg.)
Coolant	H_2O	H_2O	Terphenyl	CO_2	CO_2	H_2O	H_2O	CO_2	H_2O
Inlet temp., °F	497	478	623	423	500	508	Intermed.	536	498
Outlet temp., °F	519	616	660	752	896	565	Heat exch.	932	537
Pressure, psi	1750	2940	40 (max.)	300	800	1845	800	570	1986
Circulation rate	19,800 gpm	4400 gpm	15×10^6 lb/hr			8400 gpm	8400 gpm	200 tons/hr	30,000 gpm
Steam rate, tons/hr	121	360†	165			116	98	80	240
Temp., °F	462	590	Sat'd.	700	940	Sat'd.	Sat'd.	450	482
Pressure, psia	475	400	800	500	1030	600	650	650	570
Weight data									
Reactor system, tons	600	1054	500						528
Contain. and shield, tons	1900	1963	1000						2550
Propulsion mach., tons	1150	2750	1100						1760
Nom. SHP	20,000	44,000	30,000	50,000	50,000	18,000	18,000	18,000	44,000
Life at power	730 days	1 year				2 years			420 days

* Estimated.

† All reactors operating.

The primary shielding consists of 33 in. of light water and 3 in. of lead around the pressure vessel. The secondary shielding surrounds the containment vessel and consists of 6½ in. of lead and 6½ in. of polyethylene covering the top half of the vessel, a 4-ft-thick vertical concrete wall around the lower sides of the vessel and a 5-ft thickness of salt water ballast and feed water tanks under the bottom of the vessel.

The reactor is protected against collision damage by a collision mat consisting of a vertical wall of alternate layers of 1-in.-thick steel and 3-in.-thick redwood around the concrete shield wall. The mat appears to be between 2 and 3 ft thick.

The Savannah is being built for a fixed price (conventional practice for shipbuilders) including the ship and nuclear power plant. The total capital cost excluding the fuel but including some research and development is approximately $30,500,000 and is composed as follows:[3]

Reactor and power plant	$14,500,000
Shielding and containment	1,500,000
Hull and outfit	14,500,000

The design studies listed in Table I-1 cover a range of proposed applications as well as a range of reactor types. The Japanese, for example, have considered the use of a 44,000 SHP, 20,100-ton gross (29,070 tons displacement), nuclear-powered vessel to carry emigrants from Japan to South America.[6] Comparing the cost of a PWR powered vessel to a conventional ship they concluded that, over a 20-year period of operation, the financial rate of return for the nuclear vessel would be a factor of 2 lower than that for a conventional vessel (nuclear 17 per cent vs. conventional 34 per cent).

The British studies[7] (Table I-1) report results of an economic comparison of a conventional with a nuclear-powered supertanker. Although power plant capital cost was between 1.5 and 2 times that required for a conventional shipboard power plant, the specific fuel cost (dollars per SHP hour) was less for nuclear-powered vessels in excess of about 25,000 SHP. The operating costs for nuclear-powered vessels showed that, for fuel oil at a cost of 8 cents/gal, the nuclear ship broke even (based on operating costs) at a cargo deadweight of about 73,000 tons for a nuclear fuel burn-up of 2700 Mwd/ton. Increasing the burn-up to about 5400 Mwd/ton decreased the break-even cargo deadweight to 44,000 tons.

Atomics International[9] has studied the use of an organic-moderated reactor (OMR) in a 20,000 SHP, 38,000 deadweight ton tanker. The vessel sails from Kuwait to Philadelphia via either the Suez Canal or the Cape of Good Hope. The report considers two reactor systems and the figures given here and in Table I-1 apply to the more advanced, or subsequent, reactor—"assuming several other similar maritime OMR plants have been constructed so that engineering costs are diminished." The complete vessel cost for the OMR powered system was about 25 per cent greater than that for a conventional vessel. Operating costs were a function of route. The nuclear tanker traveling via the Suez Canal route operated at a cost about 14 per cent higher than that of the conventional ship; for the voyage around the Cape of Good Hope the operating costs were about the same.

American-Standard Study

By far the most extensive analytical study of nuclear ship propulsion has been made by American-Standard.[1] Four different reactor types were studied over ranges of size, application, and trade route variables, and economic predictions were made as of the year 1957 and for 1965 and 1970. The entire analysis covered some 30,000 individual cases. Some of the main conclusions are quoted in the following:

1. Nuclear ships can economically compete now with conventional ships on long trade routes at high speeds.
2. The competitive position of nuclear ships will improve in 1965 and 1970.
3. Nuclear fuel costs are, in most instances, lower than conventional fuel costs.
4. Nuclear ship capital costs are 10 to 50% higher than capital costs for conventional ships (except for gas-cooled reactor powered ships).
5. Capital costs for nuclear ships will decrease with respect to capital costs for conventional ships in 1965 and 1970.
6. Ore carriers and tankers have the best potential for the economic application of nuclear power to merchant ship propulsion.
7. Nuclear power is particularly attractive in trades that require small ships on long trade routes.

Within the framework of current maritime practice, ore-carriers have the greatest area of economic potential for nuclear propulsion. Valuable cargo tonnage in nuclear ships of this type is not sacrificed for fuel space. In addition, this type of ship is usually large and requires a large amount

of power, which nuclear plants can provide at a relatively low fuel cost.

Ore carriers powered with organic-moderated or boiling-water reactors in 1957 can move cargo on 16,000- to 20,000-mile round trip routes at 19 to 22 knots at the same unit cargo cost as conventionally powered ships. By 1965, large nuclear ore carriers operating at 21 to 22 knots on long trade routes will be able to carry cargo at about nine-tenths the unit cargo cost incurred by counterpart conventional ships at the same speed. Moreover, these large nuclear ships will be competitive on a cost per ton basis at 18 to 19 knots on the long trade routes, and at 19 to 20 knots on routes as short as 12,000 miles round trip. Further improvement in the competitive position of the nuclear ships occurs in 1970.

After ore carriers, tankers are the next promising application for nuclear power in merchant ships. Large nuclear tankers in 1957 can carry cargo on 20,000-mile round trip routes at lower unit cargo costs than conventionally powered tankers, at speeds greater than 22 knots. In 1965, the area of competitiveness for such ships will begin at 12,000-mile trade routes. By 1970, nuclear tankers will be more economic than conventional ships on 20,000-mile trade routes at any speed over 17 knots, and the larger nuclear tankers will be economically attractive on routes as short as 8,000 miles round trip.

Third and fourth in order of economic attractiveness are nuclear general-cargo ships and nuclear passenger ships.

The particular nuclear propulsion systems which offer the earliest opportunity for achieving a competitive position with fossil-fueled powered plants are the organic-moderated and boiling-water reactor systems. In all the cases mentioned above, these two types of reactor propulsion systems are the ones that are able to compete with conventional vessels. Both reactor types present a promising potential for the early economic introduction of nuclear technology into the field of merchant ship propulsion. From the standpoint of their comparative developmental status, the most attractive system for nuclear ships in the immediate future is the boiling-water reactor, and the most attractive system for the near future is the organic-moderated reactor.

The conclusions summarized above are, on the whole, quite encouraging. There is some uncertainty as to the implication of the estimates for "present" reactors, for it is stated that the reactors are assumed to be fully developed for the application considered and that this development would require some further work beyond that which has been done to date. Perhaps the most informative results for the reactor designer are those which specify the major performance and cost characteristics of the reactors which were arrived at in the study. These may be considered as targets which must be attained if the economic relationships predicted in the study are to hold. Some of these characteristics are given briefly below.

In the case of the ore carrier, which was judged to be the most promising application, the nuclear reactor and machinery cost for a boiling water plant of 45,000 SHP was estimated to be $13,000,000 or $289 per SHP. This corresponds to $387 per kw(e) if the power output is converted to electrical units. This cost applies to a natural circulation plant provided with a containment structure which would contain all the primary coolant in the event of a rupture of the reactor primary system.

Again for the case of the boiling water reactor in 1957, the fuel cost is estimated to consist of a unit variable cost of 0.92 mill/kw(t)-hr plus a fixed cost (inventory) of $720 per day (for a plant of 45,000 SHP). These estimates are based on a fuel lifetime of 10,000 Mwd/ton and cylindrical UO_2 elements with stainless-steel jackets. A fuel fabrication cost of $13 per pound of uranium (from UO_2 powder to finished elements) is estimated. A plutonium buy-back price of $30 per gram is also assumed. The plant, operating at 800 psia, gives a thermal efficiency of 32.1 per cent.

At the power level of 45,000 SHP, the operating weight of the plant including reactor, containment, shielding, and propulsion machinery, again for the boiling water reactor, is estimated at about 70 pounds per SHP. This figure may be compared with that of 365 pounds per SHP for the N. S. Savannah.

With respect to reactor types, the study did not show great differences between the pressurized water, boiling water, and organic-moderated types; only the gas system, which employed a gas turbine, was more expensive by a large fraction. All of the reactors studied employed partially enriched fuel (except one family of pressurized-water reactors which was investigated with fully enriched fuel). Both the pressurized water and boiling water reactors used fuel elements composed of steel-jacketed UO_2 pellets. The organic-moderated reactor was designed with metal fuel elements, jacketed in aluminum. The life expectancy in this case was only 3,000 Mwd/ton, but the

rather high conversion ratio attained, along with the $30 plutonium price, made the fuel cycle competitive. The cost of organic make-up contributed about 0.12 mill/kw(t)-hr to the power cost. The gas-cooled reactor employed graphite moderation and steel-jacketed UO_2 fuel. The coolant (and turbine working fluid) was helium. It was stated that the induced radioactivity in CO_2 would require shielding of the propulsion machinery and would result in a weight penalty of 150 to 400 tons over the reactor power level design range of 10 to 200 thermal megawatts.

Hazard Considerations

The hazards peculiar to nuclear systems affect the outlook for nuclear ship propulsion in a number of ways. The first and most obvious effect is the present uncertainty as to the general acceptance of nuclear ships by national and local port authorities outside the United States. Unless such acceptance is well established the ownership of a nuclear ship will be a risky financial venture regardless of other economic factors. Presumably the primary use of the N. S. Savannah will be to establish precedents for the acceptance of nuclear-powered ships in foreign commerce.

A second question related to hazards is that of the cost and availability of third-party liability insurance. In the American-Standard study[1] the total insurance charges were said to be 60 to 100 per cent higher for nuclear than for conventional ships, and to constitute from 12 to 13 per cent of the total daily fixed charges. However, it cannot now be said that reliable estimates of insurance costs can be made. The problem of insurance for nuclear vessels is being studied by the Nucleonics Committee of the American Institute of Marine Underwriters.[10]

Finally, hazards considerations and the degree to which precautions are taken affect the capital cost of the nuclear ship. The N. S. Savannah, with a separate containment vessel and collision mats around a relatively low-power-density reactor, probably represents the practical limit to which safety precautions can be carried with the pressurized-water reactor. These precautions undoubtedly add substantially to the cost and weight of the plant. It has been stated in reference 3 that according to recent design studies there is good assurance that ship structure can provide adequate protection against the release of radioactivity without the use of a separate containment vessel, and that this question of the containment feature will become pivotal in the development of truly economic nuclear ships.

References

1. D. L. Conklin et al., Economics of Nuclear and Conventional Merchant Ships, ASAE-S-5, June 1958. (Unclassified AEC report.)
2.* Michiya Shigemitsu, Nuclear-powered Submarine Tanker, A/CONF.15/P/1320.
3.* W. H. Zinn and R. P. Godwin, The Use of Nuclear Energy for Purposes Other Than the Generation of Electricity, A/CONF.15/P/1831.
4.* N. S. Khlopkin, Atomic Icebreaker "Lenin," A/CONF.15/P/2140.
5.* R. P. Godwin and D. L. Worf, Design Considerations in Nuclear Merchant Ships, A/CONF.15/P/1023.
6.* S. Takeuchi, T. Okamura, and S. Murakami, Nuclear Powered Emigrant Ship, A/CONF.15/P/1319.
7.* R. V. Moore and C. E. Iliffe, Nuclear Propulsion for Ships, A/CONF.15/P/266.
8.* J. Hainzelin et al., Possibilities and Conditions of Use of Water or Gas Type Reactors in a Tanker, A/CONF.15/P/1137.
9. Economic Analysis of an OMR-Powered 38,000-DWT Tanker, NAA-SR-1879, March 1957. (Unclassified AEC report.)
10. C. G. Cornwell, Nuclear Powered Ships for American Ship Operators, TID-7539, September 1957. pp. 51-57. (Unclassified AEC report.)

* Second United Nations International Conference on the Peaceful Uses of Atomic Energy, Geneva, September 1958. (Available from the Office of Technical Services, Dept. of Commerce, Washington 25, D. C.)

Reactor Physics Constants

Reference 1 is the first publication of the Reactor Physics Constants Center, which is located at Argonne National Laboratory. The primary objective of the Constants Center is stated to be the periodic compilation of the latest and best values of the constants, recipes, formulas, etc., which are necessary to calculate reactor characteristics. The compilations, as reported by this initial one, which covers data available up to Mar. 15, 1958, and some later data, are to be quite comprehensive and will undoubtedly become the first recourse of the reactor design physicist. The scope of the work can best be summarized by a list of major subdivisions: Fission Process, Selected Cross Section Data, Constants for Thermal Homogeneous Reactors, Lattice Constants for Thermal Heterogeneous Systems, Intermediate Reactors, Fast Reactors, Shielding Constants, Constants Related to Interpretation of Experimental Data, and Properties of Elements and Reactor Materials.[1] Obviously the magnitude of the task of arriving at "best" values for the various constants, recipes, and formulas requires that this part of the objective of the Center must be a long-term one. However, the work accomplished to date, as represented by this first report, is highly useful, and the activity of the Center fills an obvious need in the reactor program.

Neutron Slowing Down

A number of recent papers have given new experimental and theoretical information on neutron slowing down. Most of the information consists of values of the age for neutrons of various initial energy distributions in various moderators. However, reference 2 is a review of the subject of slowing down in hydrogenous moderators.

Hydrogenous Moderators

The pursuit of the classic discrepancy between theory and experiment in the slowing down of fission neutrons in hydrogenous media is continued in reference 2, which summarizes developments in this area since the review paper of the 1955 Geneva conference.[3] The following section is a condensation of the first part of that report and can give only a rather qualitative picture of the subject. Reference 2 and its references (some of which are repeated here) should be consulted as a critical review of the subject.

The unweighted average of three measurements[4–6] of the age to indium resonance energy of fission neutrons in light water is $\tau = 30.5 \pm 1$ cm^2,* whereas the calculated values are distributed as $\tau = 26.0 \pm 0.5$ cm^2. Thus the calculations consistently result in values that are low by about 13 per cent on the average. No reasonable permutation of theoretical assumptions and approximations seems to have any significant effect on this discrepancy, and sources of experimental error have been diligently pursued and carefully evaluated. However, some sources of experimental error have been only recently considered and no uniform manner of treatment of them has yet evolved. These include:

1. *Perturbation by the Source Backing.* After examining some representative modes of treatment of this boundary effect, the authors[2] conclude that the results of the U. S. measurements, and probably those reported in the USSR, have been adequately corrected in this respect.

2. *Source Perturbations*

Geometric transformations: The authors[2] conclude corrections are adequate.

Displacement of medium by source: The authors[2] conclude the effect is small.

Source absorption and scattering: Not significant.

*An age of 27.65 cm^2 was recently measured by R. C. Doerner and F. H. Martens (ANL) and reported in a paper, Age of Fission Neutrons in Water, at the December 1958 meeting of the *American Nuclear Society*, Detroit, Mich. Their results, a summary of which is given in *Transactions of the American Nuclear Society*, 1(2): 30 (December 1958), appeared too late for inclusion in this discussion.

Source perturbation of background: Only reference 4 explicitly states correction.

3. *Detector Perturbations*

Self-shielding of black foils, leading to increased proportion of higher resonance activations: Corrections appear to be adequate.

Current-to-flux transformation: Flux age *higher* than measured current age by ~ 0.5 cm^2.

Finite cadmium cross section at indium resonance:

$$\tau_f - \tau_{exp} \sim 0.6 \text{ cm}^2$$

The authors[2] conclude that corrections for detector effects are all in the undesired direction and barely significant experimentally.

Sources of error are examined in the several "rigorous"* analytical methods that exist for computing age from a point isotropic source in an infinite homogeneous medium. Truncation and round-off errors and statistical uncertainties (in a Monte Carlo calculation) can be made as small as desired, and are currently an order of magnitude smaller than the discrepancy between theory and experiment. Unknown errors also arise from uncertainties in input data (cross sections and spectra of source neutrons).

The Monte Carlo method has been added to the Fourier transform and moments methods presented at the 1955 Gevena conference.[3] The net effect, however, is to leave the 1955 theoretical age values unchanged. The transformation for slowing down density age to flux age is derived, and the detailed assumptions, corrections, and input data used by various workers are discussed. In particular, values of oxygen total cross sections and average cosine of the scattering angle in the center-of-mass system (μ) have been revised[7] over the 1953 values[8] in general use at the time of the 1955 Geneva conference. Changes in orbital angular momentum assignments for two of the resonances have radically altered the μ curve near those resonances. These revisions have changed its sign between resonances from predominantly negative to predominantly slightly positive. The net effect on age, however, is small.[9]

Further work on oxygen cross sections above 2.5 Mev is still badly needed; however, a calculation[10] on the basis of an interim compilation[7] of oxygen cross sections from 0 to 18 Mev, based on all currently available data but with inelastic scattering counted as an absorption, has not altered the 1955 value for the theoretical age. A Fourier transform analysis[11] using an independent evaluation of the oxygen data and including inelastic scattering likewise leads to the same result. The authors[2] conclude that refinements of the oxygen data are unlikely to alter substantially the calculated age.

Although the hydrogen scattering cross section is definitely anisotropic at 14 Mev, the low-energy data are generally interpreted as indicating isotropy. These data are sufficiently rough, however, to be consistent with a 10 per cent "anisotropy factor," δ, where

$$\delta = \frac{\sigma(0)}{\sigma(\pi/2)}$$

as measured in the center-of-mass system. For a symmetrical angular distribution in the center-of-mass system, as indicated by the 90-Mev data, the average cosine of the angle of scattering in the laboratory system, α, is increased by 0.0127δ. Furthermore, considerations of nuclear forces indicate complete isotropy below 5 Mev. The authors[2] conclude that the net effect on the age of anisotropy of the scattering angular distribution must be imperceptible.

Uncertainties in the fission spectrum are shown to be inadequate to account for the discrepancy between theoretical and experimental age. Moments method calculations[9] of truncated spectra indicate that the discrepancy can be eliminated only by neglecting all neutrons below 600 kev, or about 20 per cent of the total. A perturbation approach[12] shows that the variational derivative of the flux age, τ_f, with respect to the source spectrum, N(E), is

$$\frac{1}{\tau_f} \frac{\delta \tau_f}{\sigma N(E)} = \frac{\tau(E)}{\tau_f} - 1$$

where $\tau(E)$ is the age from a monoenergetic source of energy E; an increase of 60 per cent in the spectrum above 2 Mev would be required to eliminate the discrepancy. Other types of variation lead to even more pessimistic conclusions. Methods relating the age to the *average* source energy requires 16 per cent increase in $\bar{E}$, which would be entirely incompatible with

*"Rigorous" here means that no physical assumptions or approximations are made to the Boltzmann transport equation.

available data. The largest defensible increase in $\bar{E}$ would be of the order of 5 per cent, corresponding to an increase in age of 1.3 cm^2.

In summary, the authors[2] conclude that the present values for the experimental and theoretical age of fission neutrons in water are practically equivalent to the 1955 values. The bases for the theoretical values are in essence simple and clear-cut, and the possible avenues of attack seem to have been carefully explored. The most uncertain theoretical factor is probably the shape of the source spectrum. The most significant experimental uncertainty is the absorption of the slowing-down neutrons in the source. It seems unlikely that the sum of these two effects can bridge the gap between theory and experiment.

The age for neutrons in hydrocarbon moderators is of interest in connection with the discrepancy discussed above (as well as intrinsically) because the cross-section uncertainties for carbon are less than those for oxygen. Carbon has no resonances below 2 Mev, and the angular distributions are nearly isotropic up to that energy. Preliminary measurements[15] on the age in diphenyl indicate an age of 54 ± 3 cm^2, after a correction of 8 per cent for transverse leakage. The experiments are to be repeated at higher power and with a larger tank. A Fourier-transform calculation[16] in the B_1 approximation produced an age of 46.3 cm^2, a discrepancy of the same per cent magnitude and direction as in H_2O.

A number of age determinations, in addition to those listed in reference 1, have been made for neutrons from nonfission sources. These data also are interesting as additional evidence relating to the discrepancy between theory and experiment. Reference 2 points out that these data have their own peculiar uncertainties, of a magnitude great enough to weaken greatly the strength of any conclusions that might be drawn from them. Nevertheless the reference observes that the general better agreement between theory and experiment for these sources suggests that the discrepancy for fission neutrons in water may be rooted in some peculiarity of a uranium fission source. The data on the nonfission sources are summarized below.

Age measurements have been made at Hanford[17] for sodium-beryllium photoneutrons in water and kerosene. This source has a spectrum of average energy 0.966 Mev, with a full width of 3 per cent of the mean energy, and thus approximates closely a monoenergetic source. A moments calculation[2] yielded an age to indium resonance of 13.25 cm^2 in water as compared to a measured value of 13.7 ± 0.6 cm^2. The age vs. source energy curve of Coveyou and Sullivan,[10] using the same oxygen data, gives a value of 14.3 ± 0.3 cm^2. No calculations have been made to check the measured kerosene value of 13.0 ± 0.4 cm^2.

The thermal migration area of the delayed neutron spectrum of N^{17} was reported by Shure and Roys[18] as 23.1 cm^2. Assuming a migration area of 8.7 cm^2 from indium resonance to thermal absorption, the age to indium is 14.4 cm^2 as compared to theoretical values of 13.6 cm^2 in the Selengut-Goertzel approximation* and 15.2 cm^2 by the "rigorous" method of Coveyou and Sullivan,[10] both using the Hayward[19] spectrum. Moments method calculations are in progress.

Two experiments were performed at the National Bureau of Standards with neutrons from a particle accelerator. One used the 250-kev D-D reaction[20] to produce 3-Mev neutrons; the other used the D-T reaction to produce 14.1-Mev neutrons. The latter approximated a point isotropic source, but the oxygen cross sections at that energy are so uncertain that the experiment did not make possible a fair test of theoretical calculations. The measured age was 150 ± 6 cm^2. Coveyou and Sullivan[10] computed an age of 170.4 ± 3.5 cm^2 at 13.6 Mev counting all nonelastic collisions in oxygen as absorptions. Using somewhat different but unspecified oxygen data, Reier et al.[11] computed ages of 130 cm^2 including inelastic scattering and 185 cm^2 with zero inelastic scattering.

The D-D experiment[20] was complicated by the anisotropy of the source in both intensity and energy and by the presence of the beam-tube of the accelerator. Comparable theoretical results do not exist, but a Monte Carlo calculation of the flux at 90° to the particle beam, including the effect of the evacuated beam tube, is in progress.[21] This calculation should be directly comparable to the experiment.

Measurements[5,11,22] of the age to indium resonance energy of the broad-spectrum Po-α-Be source in water give an average age of 56.3 cm^2, as compared to computed values[11] of 53.5 cm^2 and 58.2 ± 1.8 cm^2, the latter obtained[2] by aver-

*Calculations by R. L. Hellens.

aging monoenergetic ages[10] over a Murray[23] spectrum. The theoretical values differ by 5 per cent below and 3 per cent above experiment, respectively, even though uncertainties in source spectrum and oxygen cross sections exist in intensified form. Measurements of average spectrum energy vary by as much as 20 per cent, yet a Fourier transform calculation[11] in the P_1 approximation using the MUFT code and four different spectra led to a variation in age of only 2 per cent. Furthermore, 50 per cent of the Po-Be neutrons are above 4 Mev in energy, where knowledge of oxygen cross sections is sketchy, whereas only 10 per cent of fission neutrons exceed this energy. In addition, the manner of treating disappearance processes and inelastic collisions led to a 10 per cent variation in τ, whereas the use of two different sets of oxygen data produced[10] a 9 to 11 per cent variation in τ at 3.6 and 4.7 Mev. In the face of uncertainties of this magnitude, it cannot be claimed that there is any discrepancy between theory and experiment for Po-Be neutrons in water.

The measured[5] age of 148 cm^2 for Po-Be neutrons in 99.4 per cent D_2O compares well with the calculated[10] age of 150 cm^2, although the assumption of isotropic scattering in the center-of-mass system at all energies suggest chance agreement.

Measured values[11] of Po-Be neutrons in water-metal mixtures agree well with MUFT values except for zirconium-water mixtures, where the knowledge of zirconium inelastic cross sections is poor. Incidentally, the measurements indicate that volume for volume, iron is almost as good a moderator as water, due to inelastic scattering.[2]

The neutron spectrum of the Po-α-B source is poorly known but is considerably narrower than that of Po-α-Be.[2] The theoretical age in water[24] for various spectra ranges from 30 to 36 cm^2, vis-a-vis a measured age[24] of 39.7 ± 1.2 cm^2, while that in a 2:1 Al-H_2O lattice[25] varies from 109 cm^2 to 123 cm^2 vs. a measured age of 130 ± 3.9 cm^2. Thus a discrepancy of the same order of magnitude and sense exists for the Po-B-H_2O situation as for the fission case.

D_2O-H_2O Mixtures

The age in mixtures of D_2O and H_2O is of considerable practical importance in the design of D_2O-moderated reactors where the possibility of contamination of the D_2O by H_2O exists. Measurements have been reported for mixtures containing from 99.8 per cent D_2O[13] to as low as 48.6 per cent D_2O.[5] For the mixtures containing small percentages of H_2O the age is very sensitive to the H_2O content, decreasing by about 4 cm^2 for 1 per cent increase in H_2O content. When the H_2O content becomes large the age changes only slowly with composition. By the time the H_2O content has been increased to 51.4 per cent the age to indium resonance has dropped from a value of about 109 cm^2 (for 99.8 per cent D_2O) to 38.6 cm^2, which is higher by only 8 cm^2 than the value for pure H_2O.

Existing theoretical calculations[2–14] of the age for pure D_2O give results somewhat higher than measured values, probably because the preferentially backward scattering by deuterium was not taken into account. The calculated values for D_2O-H_2O mixtures are in agreement with experiment at about 60 per cent D_2O content, and, of course, fall below experiment for pure H_2O.

Graphite and Graphite-Bismuth Mixtures

The age to indium resonance for fission neutrons has been reported,[26] from exponential experiments, as 285.33 ± 0.4 cm^2 for graphite of density 1.674 g/cm^3. This would correspond to a value of 311 cm^2 for graphite of density 1.60 g/cm^3 and may be compared to the value from the Reactor Handbook[27] of 312.5 ± 0.5 cm^2 for graphite of that density. A value of 449.8 ± 2.0 cm^2 has been reported[17] for a graphite-bismuth stack, having a graphite-bismuth volume ratio of 2. The graphite density was 1.674 g/cm^3, and the stack contained some aluminum in the form of a foil wrapping for each bismuth bar. This measurement is useful in connection with the design of liquid-metal fuel reactors.

Monoenergetic Neutrons in Iron and Stainless Steel

Roos[28] has recalculated Horton's[29] ages to thermal with recent cross-section data[30] and finds that the sharp decrease in cross section at 27 kev in pure iron leads to increases by a factor of 2 in the age to thermal for source energies in excess of 27 kev. The factor could well become larger as experimental resolution of the cross-section "window" improves. In stainless steel, the window is partly covered by the alloying elements, and the changes over Horton's values are much less drastic.

Physics of Low-enrichment Light-water Reactors

The physics of the light-water-moderated and -cooled power reactor has been the subject of rather extensive experiment and analysis. Although a considerable amount of research and development has been on a prototype basis and, as such, the information does not have general application, there is at present a large body of experimental data available against which methods of analysis can be tried.

Recent papers have summarized the status of theory and experiment for light-water lattices[33] and the application of digital-computer techniques to the calculation of light-water-moderated reactors.[51] A digest of this material is beyond the scope of the present review, but the following section will serve as a guide to the current sources of experimental and theoretical information.

Experimental

During the past few years, experimental techniques have been greatly improved, and rather difficult measurements are now made in routine fashion. Further, there has been a greater emphasis on the performance of experiments that lend themselves directly to prescribed analytical methods. Much of the experimentation on H_2O-moderated lattices has been done at Brookhaven National Laboratory (BNL) and at the Westinghouse Atomic Power Division (Bettis).

The BNL experimental measurements on metallic rod lattices have been described in references 31, 32, and 33. Fuel rods with 0.250, 0.387, and 0.600 in. diameters, clad with 0.028-in. 2S aluminum, with a nominal 0.005-in. air gap between fuel and clad, have been positioned such that the water-uranium volumes ranged from 1 to 4. The U^{235} enrichments studies (by weight) were 1.027, 1.143, and 1.299 per cent.

The experimental data at Bettis have been obtained by critical assembly techniques.[34–36] Measurements were performed on the identical metallic rods used in the BNL experiments for the 0.387- and 0.600-in. cases with 1.143 and 1.299 per cent enrichments. Also, oxide measurements were made for 1.311 per cent enrichment with UO_2 density 7.52 g/cm^3 and 10.53 g/cm^3. The oxide fuel diameter was 0.385 and 0.601 in., and the water to oxide volume ratio ranged from 1 to 2.5.

For all the lattices described above, buckling measurements have been made, as well as determinations of lattice parameters, including fast effect, resonance escape probability and disadvantage factors. In addition, measurements of reflector savings, migration areas, and temperature coefficients were made in the temperature range 20 to 50°C.

A set of measurements was also made at BNL[33] on lattices whose fuel was 1 per cent plutonium, 0.3 per cent U^{235}, and 98.7 per cent U^{238}. The rods were 0.387 in. in diameter and were clad like the slightly enriched lattices mentioned above.

Zero-power experiments have been performed on the EBWR reactor.[37] These experiments include four different plate type uranium-metal fuel elements of two-plate thicknesses and in two enrichments. One plate is 0.214 in. thick, and the other is 0.279 in. thick; both are clad with 0.020-in. Zircaloy-2. The two enrichments are natural uranium and 1.44 per cent enriched uranium. The measurements reported include critical mass determinations, control rod calibrations, void and temperature coefficient measurements, determinations of reactivity compensated by steam voids, and the effect of boric acid and control rods on power generation.

Extensive measurements have been made on the Shippingport reactor[38] utilizing zero-power mock-up facilities.[39–40] The geometrical configuration consisted of a seed and blanket. The seed was composed of zirconium plates assembled into subassemblies approximating the mechanical design of the PWR seed. The seed fuel, in the form of enriched uranium oxide, was dispersed in plastic tape and cemented to the zirconium plates. The blanket material consisted of natural uranium oxide pellets, identical to those used in PWR, inserted into aluminum tubes having approximately the dimensions of PWR blanket fuel assemblies. The principal measurements in the mock-up facility comprised determinations of critical configurations, excess and shutdown reactivities, power distributions, and temperature coefficients.

Zero-power experiments on a mock-up of the Yankee Atomic Power Plant[41] have recently been performed.[42–44] The fuel rods consisted of 0.300-in.-diameter UO_2 pellets sealed in type 304 stainless-steel tubing with a wall thickness

of 0.016 in. The U^{235} enrichment is 2.7 wt.%. The fuel rod spacings were varied to give water-to-fuel volume ratios from 2.23 to 3.81. Measurements of critical size, buckling, reflector savings, migration area, disadvantage factor, resonance escape probability, and temperature coefficient were made for each core.

Experiments similar to the Yankee plant have been performed on the Savannah Merchant Ship.[62] The fuel consists of UO_2, enriched to 4 per cent U^{235}, in the form of 0.500-in.-diameter rods with a 0.028-in. stainless-steel clad. The fuel has been arranged in critical arrays with water to UO_2 volume ratios[63] of 1.15 and 1.54.

As a part of the Russian program on pressurized-water reactors[45] measurements of lattice parameters and bucklings for metallic rods of approximately 1.35 in. in diameter have been made for water to uranium volume ratios[46] ranging between 0.4 and 2.0. For the latter experiments spiked and seed-blanket arrangements were also measured. Measurements of the neutron spectrum in uranium-water lattices were also made for the 1.35-in. rods.[47] Apparently these experiments, with large metallic rods, were made for general information; the Russian pressurized water designs employ oxide elements of relatively small diameter.

Experiments have been performed in the United States on several enriched uranium-thorium-water critical assemblies[48] in connection with the Consolidated Edison Reactor design. These experiments have included both plate type elements containing thorium metal and pin type elements containing thorium oxide. Lattice parameters, critical masses, and bucklings and migration areas were determined for both types of assemblies for several uranium-to-thorium ratios.

Organic materials such as diphenyl have moderating properties quite similar to those of light water reduced to an equal hydrogen density. Exponential experiments have been performed with lattices consisting of 1-in.-diameter metallic uranium rods in liquid diphenyl.[49] The fuel used consisted of both natural uranium and 0.912 at.% U^{235}. For each enrichment, lattices of moderator-to-fuel volume ratios ranging from 1.5 to 4 were studied. Measurement of bucklings, age, and diffusion lengths were made.

In addition to the lattice experiments described above, the recent revised cross-section compilation[50] is of course pertinent to the subject. Further, measurements in the fields of neutron spectra, reactor control, and reactor kinetics are also important. Much of the recent information on these subjects is summarized in the Argonne National Laboratory Reactor Physics Constants compilation.[1]

Theoretical

The "classical" formulation of the theory for heterogeneous thermal reactors was developed for well thermalized lattices. Slightly enriched H_2O-moderated lattices, of compositions which can attain criticality, are in general not well thermalized; i.e., an important fraction of the fissions is caused by neutrons of epithermal energy, and the thermal-neutron energy spectrum is determined by the ratio of absorption to moderating power as well as by the temperature of the moderator. Other peculiarities of H_2O-moderated lattices are the relatively important fast-fission effect, involving interactions between fuel lumps, and the non-Gaussian spatial distribution of the slowing-down density. As a result of some of the peculiarities, the theoretical bases for expecting the approximations involved in the "four-factor" formulation to be good ones no longer exist (although reference 33 states "It may however be stated that a previous conclusion [see reference 32] still seems valid: A four-factor interpretation is self-consistent if the values of η which are used are those based on a choice of 1.309 for natural uranium"). Consequently the current theories for H_2O-moderated lattices do not involve the four-factor approximation. Reference 33 gives a review of the basic approach used in most of the current calculational schemes. Salient points of the approach are

1. The theoretical treatment begins from a spherical P_1 approximation to the transport equation, which deals with homogenized neutron properties and contains self-shielding factors to allow for those features which homogenization would ordinarily suppress (higher approximations to the transport equation may of course be used to calculate the self-shielding factors).

2. The energy distribution of the neutrons is treated by few-group theory—a multigroup theory comprising a relatively small number of groups. Fission and absorption are allowed in all groups; hence, the limitations of the four-factor formulation, which conceptually restrict the processes of fast fission, resonance absorp-

tion, and thermal absorption to specific energy regions, is avoided. It is stated that often two, three, or four energy groups appear to be adequate for most design purposes. For such broad groups cross coupling of the groups can be neglected. The few-group constants may be arrived at by solving a simplified problem by many-group theory and choosing the few-group constants to be consistent with the resulting energy spectrum. Other papers on the computation of group constants are references 52, 53, and 54.

3. Thermal neutrons are treated by one-group diffusion theory; the top energy of the thermal group is chosen sufficiently high that no scattering out of the group occurs. The thermal-neutron energy spectrum is determined by a calculation, such as the Wigner-Wilkins, which takes into account the equilibrium between absorption and moderation. Usually this calculation is made by machine, using a code such as SOFOCATE, which has the advantages over the Wigner-Wilkins method of allowing absorption cross section variations other than 1/v, and of accounting for neutron leakage.

Reference 85 gives a rather detailed description of the set-up of a five-group model for H_2O-moderated lattices, the five-group model being derived from a 22-group analysis. The model is applied to several lattices for which experimental data are available, and comparisons are made with experimental results.

Although the basic theory of the reactor is of fundamental importance, much of the theoretical and computational effort on H_2O reactors has gone into the solution of practical design problems which owe their difficulty to their complexity. Typical problems are the prediction of the variation of the spatial power distribution over the life of the core, the prediction of reactivity lifetime when the fuel burn-up is nonuniform, and the calculation of temperature and void coefficients of reactivity for nonuniform cores. Many of these problems have been attacked by machine computation. A review of the role of the digital computer in the design of water reactors is given in reference 51. The codes for predicting reactivity behavior solve the multi-group diffusion equations. Many one-dimensional diffusion codes are now in use. These codes include WANDA,[55] PROD,[56] and GNU.[57] CANDLE[58] and BOX are one-dimensional codes that include composition changes due to the burn-up and buildup of different isotopes. Two two-dimensional codes that are now in operation are CURE[59] and PDQ.[60] These codes also include provisions to calculate composition changes as a function of lifetime. TRIXY[61] is a three-dimensional code now in operation. TKO and FLAME are three-dimensional codes which are now being developed.

Doppler Coefficient for U^{238}

In reactors which utilize low-enrichment uranium as fuel, the temperature coefficient of the effective resonance integral for U^{238} is a predominant factor in the prompt temperature coefficient of reactivity. It is important in safety evaluations, and it contributes to the reactivity change between the low-power low-temperature condition and the hot operating condition. Measurements of the variation in the U^{238} effective resonance integral with fuel temperature have been carried out by several investigators. The results of the different measurements are not in good agreement relative to the accuracy required in reactivity calculations. High accuracy is especially important in calculations for reactors utilizing natural or near-natural UO_2 as the fuel because of the marginal excess reactivity available in such reactors and the high operating temperature of the UO_2. However, the order of magnitude of the effect is well established by the various measurements and also by calculations based on experimental data on the resonance structure of U^{238}. The values of dA/AdT interpreted from the various measurements range from $\sim 1.3 \times 10^{-4}$ per degree centigrade to $\sim 2.1 \times 10^{-4}$ per degree centigrade (between room temperature and about 650°C), where A is the volume-absorption term in the formulation

$$RI = \frac{A}{F} + B\left(\frac{\text{surface}}{\text{mass}}\right)$$

for the resonance integral. In this formulation, A and B are constants of the material, and F is the resonance disadvantage factor.

The results of a comprehensive set of measurements have recently been reported[64] on the temperature coefficient of the effective resonance integral for U^{238} over the temperature range 20 to 600°C for the metal and 20 to 1000°C for UO_2. The surface-to-mass dependence of the temperature coefficient was investigated by the use of fuel slugs of three different diameters,

ranging from 8 to 28 mm for both the metal and the oxide fuel. Thus it was possible, from analysis of the data, to determine the separate temperature coefficients of the two absorption terms comprising the foregoing formulation for the resonance integral. The rods were irradiated in a cadmium-covered oven in the reflector of the Swedish D_2O reactor R1. Measurements were carried out by an activation technique based on obtaining the intensity, for solutions of the irradiated samples in nitric acid, of the 105-kev X-ray line in Pu^{239} following the Np^{239} decay.

In the interpretation of the activation measurements, the temperature dependence of the effective resonance integral was taken to be of the form

$$RI(t) = RI(1/v) + \left[1 + \alpha\,(t - 20)\right]\frac{A}{F} + \left[1 + \beta\,(t - 20)\right] B\,\frac{S}{M}$$

The percentage increase in specific activity of the irradiated samples was assumed to be linearly dependent on the temperature over the temperature range investigated. Within the data scatter and the estimated probable errors for each data point, this assumption is indicated by the plotted data to be about as reasonable as any. The values given by Hellstrand[65] for A (7.8 barns for metal and 11.6 b for oxide) and B (30.2 b g/cm^2 for metal and 22.8 b g/cm^2 for oxide) and the value for RI(1/v)(1.1b) were used. On these bases, the values of α and β were obtained by a least squares fit to the reduced data. The values obtained for metal are

$$\alpha = 0.6 \times 10^{-4} \text{ per } ^\circ C$$

and

$$\beta = 2.6 \times 10^{-4} \text{ per } ^\circ C$$

The values obtained for oxide are

$$\alpha = 0.1 \times 10^{-4} \text{ per } ^\circ C$$

$$\beta = 3.1 \times 10^{-4} \text{ per } ^\circ C$$

As interpreted, the experimental results show a temperature dependence which is mainly due to the effect of the surface absorption term.

The temperature coefficients of the resonance integral obtained in these measurements are compared for U^{238} metal, on a common basis, with the results of other investigators. The reported results exceed that given by Rodeback[66] but are lower than the results of Pearce and Walker[67] and of Davis.[68]

Effect of Holes on Slowing Down and Diffusion Areas

The presence of voids within a reactor medium increases the neutron age and thermal diffusion area in the medium and hence results in increased neutron leakage from the reactor. For a uniform distribution of voids whose dimensions are small compared to the neutron mean free path in the solid medium surrounding the voids, the increased age and thermal-diffusion area can be simply obtained from the age and thermal-diffusion area values when no voids are present. The expression is

$$L^2 = L_o^2\,(1 + \phi)^2$$

with a similar expression for τ. Here τ and L^2 are the age and thermal-diffusion area, respectively, with subscript o indicating the case of no voids. The ratio of void volume to solid-material volume is ϕ.

As the dimensions of the individual void volumes are increased and become large compared with the mean free path in the solid material, the foregoing simple treatment is no longer correct. In this case, the increase in τ and L^2 due to the introduction of the voids can be substantially larger than that indicated by the simple expression. Basically, the reason for the greater increase is that the neutron transport properties are governed by the root-mean-square of the neutron flights rather than by the arithmetic mean free path in the medium. As a further result the size, shape, and orientation of the individual void volumes are important considerations.

A theoretical analysis of the increase in the migration area of neutrons in a reactor by the presence of voids was made by Behrens[69] and includes the effect of size and shape of the voids. For void geometries characteristic of the holes passing through the reactor medium for the flow of the coolant in a gas-cooled power reactor, (the most important practical case), Behrens' results are expressible as

$$\frac{L_{\perp}^2}{L_o^2} = 1 + 2\,\phi + \tfrac{3}{4}\,\frac{Qr\phi}{\lambda_t}$$

$$\frac{L_{\perp\perp}^2}{L_o^2} = 1 + 2\,\phi + \tfrac{3}{2}\,\frac{Qr\phi}{\lambda_t}$$

where

$L_{\perp\perp}^2$ and $L_{\perp}^2$ = the thermal diffusion areas parallel and perpendicular, respectively, to the gas-flow passages

λ_t = the thermal neutron mean free path in the solid medium

r = the hydraulic radius of the hole (twice the volume of the void divided by the surface area of the void)

Q = a function of the shape of the hole

A similar expression, with λ_t equal to the neutron mean free path during the slowing-down process, is appropriate for τ. The factor Q has been evaluated by Behrens[69] for various hole geometries.

Experimental results have recently been reported on the anisotropic diffusion lengths for thermal neutrons in large graphite assemblies containing void channels which simulate the gas-flow passages in large gas-cooled power reactors. Prior to operation of the G1 reactor (natural U-metal, graphite-moderated)[70] the reactor was partially loaded with fuel, the load being confined to one end of the graphite stacking and being sufficiently extensive to achieve criticality. The thermal-neutron diffusion was observed in the nonloaded end. The graphite stacking was pierced by gas-flow channels of 7 cm in diameter forming a square lattice of cells of 20-cm pitch. Measurements were also made with the channels filled with graphite of the same quality used in the stacking. The experimental results and a comparison with Behrens' theory are

$$\phi = 0.106$$

$$(1 + \phi)^2 = 1.223$$

$$L_o = 52.7 \pm 0.4 \text{ cm}$$

	Experiment	Behrens' theory
$(L_{\perp\perp}/L_o)^2$	1.504 ± 0.040	1.494
$(L_{\perp}/L_o)^2$	1.393 ± 0.045	1.353
$\epsilon = (L_{\perp\perp}/L_{\perp})^2$	1.08 ± 0.03	1.104

An experimental test of Behrens' theory is also provided by reference 71 in which a large value of $\phi = 0.333$ was used. A graphite stacking approximately 66 by 65 by 73 in. was used, and the source of thermal neutrons was obtained from a graphite pedestal with an antimony-beryllium source. Measurements of thermal neutron flux were made with and without the void channels (of square cross section) running the length of the pile. The results obtained and comparison with Behrens' theory are tabulated below.

$$\phi = 0.333$$

$$L_o = 54.7 \pm 1.8 \text{ cm}$$

	Experiment	Behrens' theory
$L_{\perp\perp}$ (cm)	94.0 ± 3.0	94.6 ± 3.1
$L_{\perp}$ (cm)	82.2 ± 2.5	83.5 ± 2.7
ϵ	1.305 ± 0.03	1.284

The two separate sets of measurements provide, for the first time, experimental confirmation of Behrens' analytical results, at least for assemblies typical of the large gas-cooled graphite- or D_2O-moderated reactors fueled with natural or near-natural uranium. These results indicate that for the relatively large assemblies used, the neutron-streaming "end effects" are small. Near the ends of the reactor assembly, a significant fraction of the neutron flights into the gas passages lie in a range of solid angles such that the neutron is not again intercepted by the reactor medium; since Behrens' analysis is for an infinite medium this end effect is not accounted for in his theory.

In reference 72 the statement is made that "the migration area asymmetry associated with the presence of large gas-cooling channels (for the Calder Hall reactor) was consistent with the Windscale observations and greater than the simple predictions of Behrens." It was later stated that Behrens' values were used, and 0.2 per cent reactivity was allowed for the underestimate of neutron leakage from the Calder Hall reactor. Since the leakage from Calder Hall is only of the order of 3 to 4 per cent, the 0.2 per cent reactivity allowance will take care of an underestimation of neutron migration area of 5 to 7 per cent. This is a somewhat larger error than is indicated by the results of references 70 and 71.

Recent Measurements on DIMPLE and GLEEP

The experimental program being carried out at Harwell using the pile oscillator facilities of DIMPLE and GLEEP is described in reference 73. The work includes measurements of (1) thermal cross sections of various purely absorbing materials of interest, including some of the important stable fission-product poisons; (2) resonance absorption integrals, of which that for Pu^{240} is of special interest; (3) η values for U^{233} and Pu^{239} relative to that for U^{235}; and (4) reactivity changes of irradiated fuel from the Windscale and NRX reactors. The results obtained to date are reported and compared with existing information.[73] Because of the importance of such basic data in reactor calculations and particularly of the measurements made in several reactor spectra, a summary of the results is given here in some detail.

In natural or near-natural uranium systems it is convenient and appropriate to use the cross-section convention and pile-spectrum characterization introduced by Westcott in reference 74. A 1958 revision of reference 74 has recently been published by Westcott.[75] In this formulation, the effective neutron cross section is so defined that its product with the "2200 meters per second flux" (i.e., flux given by the total neutron density, including the epithermal neutrons, multiplied by v_o = 2200 meters per second) gives the correct reaction rate directly. Obviously, such a formulation is useful only if the epithermal contribution is not large; this is usually true in natural uranium or near-natural uranium systems. On this basis, the effective cross section $\hat{\sigma}$ is given by

$$\hat{\sigma} = \sigma_o (g + rs)$$

where σ_o = 2200 meters per second cross-section value

g = a measure of the departure of the cross-section variation from the 1/v behavior in the thermal region (for a 1/v absorber, g = 1)

$$s = \frac{4T}{\sqrt{\pi T_o}} \frac{\sigma_r}{\sigma_o}$$

with T the neutron temperature, T_o = 293°K, and σ_r the resonance integral excess over 1/v (for a 1/v absorber, s = 0)

r = a measure of the ratio of the epithermal to thermal neutron densities

In this formulation, epithermal flux is assumed to be distributed in energy as 1/E; hence, again, the applicability only to systems of low epithermal component is apparent.

From measurements in a pure Maxwellian spectrum ($r \sim o$), $g\sigma_o$ is obtained directly. From further measurements in a neutron spectrum with a known epithermal component (as given by the value of r), σ_r can be deduced from the difference between the two results.

In DIMPLE, the spectrum at the sample position is extremely well thermalized ($r < 0.001$). In GLEEP, r = 0.045 at the sample position.

Values of σ_o obtained from the measurements for various purely absorbing materials compare well with BNL-325 (and its Supplement No. 1) tabulation. For the important stable fission-product Sm^{149}, however, the oscillator value is 42,100 b compared to 66,000 b as given in BNL-325. The 42,100 b value is said to be in good agreement with that recently measured[76] by a different technique. For Np^{237}, $g\sigma_o$ was determined as 169 b. Since Np^{237} has been shown to follow a near 1/v law, the measurement gives a σ_o value in good agreement with other investigators. A value of σ_o for Pu^{240} was deduced as 370 ± 40 b from measurements on a sample whose isotropic composition of Pu^{239}, Pu^{240}, Pu^{241}, and Pu^{242} was determined by mass spectrometer analysis; comparison is made in the reference with the results of various investigators.

Some of the data on resonance absorption integrals obtained in a hardened neutron spectrum in DIMPLE (r = 0.098 obtained by loading of 1.2 per cent U^{235} fuel around oscillator tube) are in conflict with those of Macklin and Pomerance.[77] For Hf, σ_r = 2800 b was measured as compared to the 1250 b value reported in reference 77. For Pu^{240}, a value of σ_r = 11,300 ± 1000 b was measured, and this value is compared in the reference with that of other investigators. The USSR parameters list σ_r (Pu^{240}) = 10,000 ± 1500 b.

Measurements of relative values of η of the fissile nuclei have also been made by the pile oscillator technique. The oscillator measurement (by comparison with a standard sample) gives σ_{eff}, which is related to the absorption cross-section σ_a and the neutron yield η by

$$\sigma_{eff} = \sigma_a (1 - W\eta)$$

where W is the ratio of the fission-neutron to thermal-neutron importance at the sample position. Because of the similarity of the fission-neutron spectra of the fissionable isotopes, W is taken to be the same for U^{235}, U^{233}, and Pu^{239}. Hence

$$\eta \propto \left(1 - \frac{\sigma_{eff}}{\sigma_a}\right)$$

where σ_{eff} is given by the pile-oscillator measurements and where appropriate values of σ_a were obtained from Westcott's compilation.[74] It is stated in the reference that uncertainties in σ_a introduce an uncertainty of about 1.5 per cent in the determination of the relative η values. The results are given in the following table with Westcott's predicted ratios for these spectrum conditions shown in parentheses.

Reactor spectrum	$\eta(U^{233})/\eta(U^{235})$	$\eta(Pu^{239})/\eta(U^{235})$
DIMPLE (~Maxwellian)	1.057 ± 0.015 (1.103)	0.974 ± 0.015 (0.987)
GLEEP	1.091 ± 0.015 (1.102)	0.980 ± 0.015 (0.962)

For U^{233}, the situation is confusing. On the basis that η (U^{235}) in the DIMPLE spectrum is expected to be not more than 0.5 per cent higher than in GLEEP, while $\eta(U^{233})$ should have the same value in both reactor spectra, the DIMPLE measurements for the η ratio should be only about 0.5 per cent lower than the GLEEP measurement. The GLEEP measurement gives reasonably good agreement with Westcott's predicted ratio; however, it is stated in the paper[73] that the use of "better data" for σ_a (U^{233}) in the analysis of the oscillator measurements would lead to a lower η ratio. The DIMPLE measurement gives an η ratio some 4 per cent lower than Westcott's predicted ratio.

The over-all absolute discrepancies in the value of $\eta(U^{233})$ are large. If an average of the DIMPLE and GLEEP measured values of $\eta(U^{233})/\eta(U^{235})$ is taken and if $\eta(U^{235})$ is taken as 2.07, then $\eta(U^{233}) = 2.22$. This compares to a value of 2.28 obtained when using Westcott's value for the ratio. However, the situation is further complicated by the suggestion in reference 78 that $\eta(U^{235}) = 2.04$, made on the basis of current interpretations of exponential experiments at Harwell; in this case, when the average of the DIMPLE and the GLEEP measured ratios is used, $\eta(U^{233})$ becomes equal to 2.19. Hence, the present uncertainty in $\eta(U^{233})$ is of the order of 4 per cent.

The situation with respect to Pu^{239} is considerably better. The DIMPLE value of $\eta(Pu^{239})/\eta(U^{235})$ is in fair agreement with Westcott's recommended 0.987 and agrees well with the value of 0.97 given by Harvey and Sanders.[79]

Reference 1 (Sec. 2) presents a detailed comparison of η values determined by various investigations for U^{235}, U^{233}, and Pu^{239}; in the comparison, plots are given of $\eta(E)$ vs. neutron energy E.

In a panel discussion at the winter meeting of the American Nuclear Society, Weinberg[80] called attention to the great significance of the η of U^{233} for the future of U^{233} breeding, and stated that a concerted effort is being undertaken in the United States to reduce the uncertainty in this constant.

GLEEP measurements have also been made for a variety of irradiated fuel materials. The results are being interpreted using a fairly simple model of neutron behavior for the purpose of deriving reasonable combinations of the pertinent nuclear constants with sufficient accuracy for predictions of long-term reactivity changes. A typical analysis is given in the paper[73] for a set of some 20 NRX uranium bars irradiated to a maximum of ~2400 Mwd/ton. In the analysis of the pile oscillator experiments, which measure the change in effective cross section of the bar with irradiation exposure, it is necessary to account accurately for:

1. The change in thermal neutron blackness of the bar with irradiation exposure.
2. The relative blackness of the unirradiated bar and the standard boron sample used.
3. The growth of Sm^{149} from the decay of Pm^{149} after reactor shutdown.
4. The over-all contribution from the fission products.

Calculations were also made of the changes in the isotopic composition of the fuel with irradiation exposure using an NRX conversion ratio of 0.76 and using effective cross sections appropriate to the spectrum conditions in GLEEP. The heavy isotope cross-section data used in the calculations were those presented in references 81 and 82. In order to convert the calculational results to reactivity contribution as interpreted

from the GLEEP measurements, a calculated value of W (ratio of fission to thermal neutron importance at the sample position) was used.

The predicted reactivity variation is in fair agreement with the measured variation. It should be pointed out that the $\eta(U^{235})$ for 2200 meters per second neutrons was taken as 2.04 in the calculations (as given by the source of cross-section data used). If a value of $\eta(U^{235})$ of 2.07 rather than 2.04 were used, the predicted curve shows appreciably less reactivity than the measured curve. This illustrates the sensitivity of the prediction to small variations in the nuclear data.

Estimated Reactivity Lifetime in D_2O Reactors

From a critical study of the changes in isotopic composition and nuclear parameters of the fuel with irradiation exposure, it is concluded in reference 83 that there is a good possibility that fuel exposures greater than 8000 Mwd/tonne* can be achieved in a large D_2O-moderated natural-uranium power reactor using fuel in the oxide form. This conclusion is pertinent to any evaluation of the D_2O-moderated reactor as a type and the methods used in arriving at the estimate are of general interest in relation to the prediction of reactivity lifetime. Obviously, the conclusion must be based on an estimate of the neutron economy attainable in a practical power reactor. The exposure prediction is based also on the use of the bi-directional fuel-push-through refueling scheme. The neutron balance, as it varies with fuel irradiation, is extremely sensitive to (1) the relative rates of depletion of U^{235} and ingrowth of Pu^{239}, Pu^{240}, Pu^{241}, and fission products (which depend on the effective cross sections of the isotopes and the rate of conversion of U^{238} to Pu^{239}), and (2) the η values for the fissionable isotopes. The effective cross sections and η values depend on the neutron spectrum seen by the "fuel" during the irradiation exposure. Uncertainties in the basic nuclear data and in properly accounting for the neutron-spectrum effects may introduce rather large uncertainties in predicted fuel exposures as limited by reactivity considerations.

In reference 83, the evidence is summarized on the basis of which the prediction of a yield greater than 8000 Mwd/tonne is made. One important piece of evidence is the agreement obtained between the results of calculations by Kushneriuk and the results of analysis of NRX rod No. 683. This natural uranium metal rod was originally installed in the NRX reactor and irradiated until the central portion of the rod had received an exposure of about 3000 Mwd/tonne. Reference 84 describes the experimental program and the analytical techniques used, which included isotopic analysis of sections of the irradiated rod. Kushneriuk's calculations treat the neutron absorption in an NRX rod, accounting for the effects of neutron spectrum seen at different cross sections of the rod and including the effect of changes in rod composition with exposure. The World-Average values for the nuclear parameters—both the 2200 meters per second values and the variation with neutron energy—were used, with some minor revisions by Westcott[74] to include more recent values. The measured initial conversion ratio (which agrees with calculation) was used both in the calculations and in the interpretation of the isotopic analyses. The effective cross sections most susceptible of accurate interpretation from the isotopic analyses are for the parasitic absorptions* $\hat{\sigma}_c$ of Pu^{239}, Pu^{240}, and Pu^{241}. The interpretation involves use of the fission cross sections $\hat{\sigma}_F$ of Pu^{239} and Pu^{241} (and other constants); however, for the relatively low irradiation exposures involved, the $\hat{\sigma}_c$ values obtained are not sensitive to the $\hat{\sigma}_F$ values (and to the other constants) used within their estimated order of accuracy. For disks P and G of rod No. 683 (~970 and 2740 Mwd/tonne exposure, respectively) the analyses give $\hat{\sigma}_c$ (239) = 411 ± 7 and 414 ± 3 barns, respectively. These compared to calculated values of 410 and 402 barns, respectively. A plot is given of the "time-average" value of $\hat{\sigma}_c$ (240) versus irradiation time since $\hat{\sigma}_c$ (240) varies significantly with irradiation exposure. Kushneriuk's calculated "time-average" curve agrees well with the data points obtained from the analyses. For $\hat{\sigma}_c$ (Pu^{241}) a value of 430 ± 20 barns was obtained from disk G. No comparison with calculations is given; however, Westcott's tabulation[75] for the spectrum appropriate to the NRX reactor (r = 0.07 where r is defined in a previous section) also gives 430 b. Because of the over-all good

*The "tonne" is the metric ton.

*The symbol $\hat{\sigma}$ designates the effective cross section according to the Westcott formulation (see the immediately preceding section).

agreement, there is increased confidence in the use of the effective cross-section values for Pu^{239}, Pu^{240}, and Pu^{241} when proper account of the neutron-spectrum effects is taken.

Another important piece of evidence relating to the predicted exposure values is based on the results of the GLEEP pile-oscillator reactivity measurements for irradiated fuel samples. The experimental results were corrected for the buildup of Sm^{149} and for the other accumulated fission-product poisons. The corrected results then give the cross-section change, in barns per initial fissile atom (bifa) due to U^{235} depletion and plutonium-isotopes production. For comparison, the reactivity variations calculated on the basis of effective cross-section values derived from Kushneriuk's calculations for the GLEEP neutron spectrum are interpreted in terms of bifa. A large discrepancy exists between the experimental and the calculated curves of bifa vs. irradiation exposure. The calculated results indicate significantly less reactivity than experiment. It is possible to force agreement by postulating "reasonable" changes in the nuclear data. For example, if $\hat{\sigma}_F(239)/\hat{\sigma}_F(235)$ is increased by 3 per cent [with $\hat{\sigma}_C(239)$ unchanged] and also $\nu(239)/\nu(235)$ is increased by 1 per cent, the calculated curve comes close to the experimental curve.

On the basis, mainly, of the foregoing evidence (and from other considerations discussed in the paper), it is concluded that the calculational scheme used should give a lower bound to the reactivity lifetime, assuming that the initial reactivity and resonance escape factor (and hence ICR) are sufficiently well established. The calculations indicate that fuel exposures greater than 8000 Mwd/tonne are possible in a D_2O power reactor fueled with natural uranium oxide.

As summarized in a previous section, the set of nuclear data adopted by the British[81,82] gave good agreement[73] of calculated and measured reactivity changes with irradiation. The use of the World-Consistent set of nuclear data (BNL-325 and its Supplement 1 plus Westcott's revisions)[74] appears to underestimate the contribution to reactivity due to the buildup of the plutonium isotopes with irradiation exposure; this contribution to reactivity for a given initial conversion ratio depends on the relative magnitudes of the nuclear parameters for the plutonium isotopes and U^{235}. However, rather small changes in the nuclear data are sufficient to give good agreement. This behavior emphasizes the delicacy of the balance between the neutron credits and debits which determine the long-term reactivity change, and the importance of accuracy in the nuclear constants if those changes are to be predicted by calculation.

References

1. Reactor Physics Constants, ANL-5800, 1958. (Unclassified AEC report.)
2.* H. Goldstein, P. F. Zweifel, and D. G. Foster, Jr., The Slowing Down of Neutrons in Hydrogenous Media—Status of Theory and Experiment, A/CONF.15/P/2375.
3. J. E. Wilkins, Jr., R. L. Hellens, and P. F. Zweifel, Status of Experimental and Theoretical Information on Neutron Slowing-down Distributions in Hydrogenous Media, *Proceedings of the International Conference on the Peaceful Uses of Atomic Energy, Geneva, 1955*, 5: 62-76 (1956).
4. L. M. Barkov and K. N. Mukhin, The Slowing Down of Fission Neutrons in Water, *Journal of Nuclear Energy*, 4(1): 91 (1956).
5. J. W. Wade, Neutron Age in Mixtures of D_2O and H_2O, *Nuclear Science and Engineering*, 4: 12-24 (July 1958).
6. J. E. Hill, L. D. Roberts, and T. E. Fitch, Slowing Down Distribution of U^{235} Fission Neutrons from a Point Source in Light Water, *Journal of Applied Physics*, 26(8):1013 (1955).
7. H. Lustig, H. Goldstein, and M. H. Kalos, An Interim Report on the Neutron Cross Sections of Oxygen, NDA-086-2, Jan. 31, 1958. (Unclassified AEC report.)
8. H. Goldstein, Fast Neutron Data for Oxygen, NDA-Memo-15C-15, Nov. 3, 1953. (Unclassified AEC report.)
9. H. Goldstein and J. Certaine, in Applied Nuclear Physics Division Annual Progress Report for Period Ending Sept. 1, 1957, ORNL-2389, Sec. 8.12, Oct. 18, 1957. (Unclassified AEC report.)
10. R. R. Coveyou and J. G. Sullivan, Oak Ridge National Laboratory, private communication to H. Goldstein, Mar. 17, 1958; cited in reference 2.
11. M. Reier, F. Obenshain, and R. L. Hellens, The Age of Polonium-Beryllium Neutrons in Various Metal-Water Mixtures, *Nuclear Science and Engineering*, 4: 1-11 (July 1958).
12. H. Goldstein, The Effect of Variations in the Fission Neutron Spectrum at High Energies on the Age of Fission Neutrons in Water, CF-57-11-42, Nov. 15, 1957. (Unclassified AEC report.)
13. R. N. Olcott, Homogeneous Heavy Water Moderated Critical Assemblies, *Nuclear Science and Engineering*, 1: 327 (1956).
14. H. D. Brown, A Monte Carlo Study of Neutron Thermalization, to be published in the *Journal of Nuclear Energy*.

15. W. W. Brown, Neutron Age and Diffusion Length Measurements in Diphenyl, NAA-SR-MEMO-1706, Aug. 24, 1956. (Unpublished AEC report); W. W. Brown, Atomics International Div., North American Aviation, Inc., private communication to H. Goldstein, P. F. Zweifel, and D. G. Foster, Jr., Aug. 24, 1956; cited in reference 2.

16. N. C. Francis, M. L. Storm, and P. F. Zweifel, Neutron Age in Diphenyl, *Nuclear Science and Engineering*, 2: 745 (1957).

17. D. G. Foster, Jr., Hanford Atomic Products Operation; cited in reference 2.

18. K. Shure and P. A. Roys, Spatial Distribution of Thermal Neutrons from an N^{17} Source in Water, *Nuclear Science and Engineering*, 2: 170 (1956).

19. E. Hayward, The Energy Spectrum of the Delayed Neutrons from O^{17}, *Physical Review*, 75: 917 (1949).

20. V. Spiegel, Jr., D. W. Oliver, and R. S. Caswell, Age to Indium Resonance for D-D Neutrons in Water, *Nuclear Science and Engineering*, 4: 546-562 (October 1958).

21. C. R. Mullin, Knolls Atomic Power Laboratory, private communication to H. Goldstein, P. F. Zweifel, and D. G. Foster, Jr.; cited in reference 2.

22. R. H. Graham et al., Migration Area of Po-Be Neutrons in Water, MTA-45, May 13, 1953. (Unclassified AEC report.)

23. R. B. Murray and J. J. Manning, in Applied Nuclear Physics Division Annual Progress Report for Period Ending Sept. 1, 1957, ORNL-2389, Sec. 10.2, Oct. 18, 1957. (Unclassified AEC report.)

24. M. Reier, The Age of Polonium-Boron Neutrons in Water, *Nuclear Science and Engineering*, 3: 374 (1958).

25.* M. Reier, The Age of Polonium-Beryllium and Polonium-Boron Neutrons in Various Metal-Water Mixtures. A Comparison Between Theory and Experiment, A/CONF.15/P/635.

26.* J. M. Hendrie et al., Slowing Down and Diffusion Lengths of Neutrons in Graphite-Bismuth Systems, A/CONF.15/P/601.

27. J. F. Hogerton and R. C. Grass, eds., The Reactor Handbook, Vol. 1, Physics, AECD-3645, p. 485, March 1955. (Unclassified AEC report.)

28. M. Roos, On the Fermi Age of Neutrons in Iron and Stainless Steel, *Journal of Nuclear Energy*, 7(3/4): (September 1958).

29. C. C. Horton, A Note on the Slowing-Down Area in Iron, AERE-RP/M-115, March 1957. (Unclassified British report.)

30. D. J. Hughes and R. B. Schwartz, Neutron Cross Sections, Supplement No. 1, BNL-325. (Unclassified AEC report.)

31. H. Kouts et al., Exponential Experiments with Slightly Enriched Uranium Rods in Ordinary Water, *Proceedings of the International Conference on the Peaceful Uses of Atomic Energy, Geneva, 1955*, 5: 183-202 (1956).

32. H. Kouts and R. Sher, Experimental Studies of Slightly Enriched Uranium-water Moderated Lattices, BNL-486, September 1958. (Unclassified AEC report.)

33.* H. Kouts et al., Physics of Slightly Enriched, Normal Water Lattice, A/CONF.15/P/1841.

34. A. Z. Kranz, Measurements of Thermal Utilization, Resonance Escape Probability, and Fast Fission Factor of Water Moderated Slightly Enriched Uranium Lattices, WAPD-134, September 1955. (Unclassified AEC report.)

35. D. Klein et al., Measurements of Thermal Utilization, Resonance Escape Probability, and Fast Effect in Water-moderated, Slightly Enriched Uranium and Uranium Oxide Lattice, *Nuclear Science and Engineering*, 3: 403-427 (1958).

36. G. G. Smith et al., Two-region Experiments in Slightly Enriched Water-moderated Uranium and Uranium Dioxide Lattices, WAPD-TM-120, March 1958. (Unclassified AEC report.)

37. J. A. Thie, EBWR Physics Experiments, ANL-5711, July 1957. (Unclassified AEC report.)

38. A. Radkowsky and S. Krasik, Physics Aspects of Pressurized Water Reactor (PWR), *Proceedings of the International Conference on the Peaceful Uses of Atomic Energy, Geneva, 1955*, 5: 229-238 (1956).

39.* A. Radkowsky and R. T. Bayard, The Physics Aspects of Seed and Blanket Cores with Examples from PWR, A/CONF.15/P/1067.

40.* S. H. Levine et al., Temperature Coefficient Measurements of Light Water Moderated Heterogeneous Critical Assemblies, A/CONF.15/P/596.

41.* W. E. Shoupp, R. J. Coe, and W. C. Woodman, The Yankee Atomic Electric Plant, A/CONF.15/P/1038.

42. P. W. Davison, Yankee Critical Experiments Reactor, meeting of the American Nuclear Society, Detroit, Mich., December 1958.

43. D. F. Hanlen et al., Neutron Flux Distribution Measurements in the Yankee Critical Experiments Reactor, meeting of the American Nuclear Society, Detroit, Mich., December 1958.

44. W. H. Bergmann, Temperature Coefficient Measurements with the Yankee Critical Experiments Reactor, meeting of the American Nuclear Society, Detroit, Mich., December 1958.

45.* S. A. Skvortsov, Water-Water Power Reactors in the Soviet Union, A/CONF.15/P/2184.

46.* S. M. Feinberg et al., Burnup of Fuel in Water-moderated Water-cooled Power Reactors and Uranium Water Lattice Experiments, A/CONF.15/P/2145.

47.* V. I. Mostovoy et al., Measurement of the Neutron Spectrum in Uranium Water Lattices, A/CONF.15/P/2152.

48.* M. C. Edlund et al., Physics of Water Moderated Thorium Reactors, A/CONF.15/P/2405.

49.* W. W. Brown, Exponential Experiments with Organic Moderated Uranium Lattices, A/CONF. 15/P/595.

50. D. J. Hughes and R. D. Schwartz, Neutron Cross Sections, BNL-325 (2nd. Ed.), July 1, 1958. (Unclassified AEC report.)

51.* E. M. Gelbard, G. J. Habetler, and R. Ehrlich, The Role of Digital Computers in the Design of Water Moderated Reactors, A/CONF.15/P/1843.

52. R. W. Deutsch, Computing Three Group Constants for Neutron Diffusion, *Nucleonics*, 15(1): 47-51 (1957).

53. H. Bohl, E. M. Gelbard, and G. A. Ryan, MUFT-4—Fast Neutron Spectrum Code for the IBM-704, WAPD-TM-72, July 1957. (Unclassified AEC report.)

54. H. Amster and R. Suarez, The Calculation of Thermal Constants Averaged over a Wigner-Wilkins Flux Spectrum: Description of the SOFOCATE Code, WAPD-TM-39, January 1957. (Unclassified AEC report.)

55. O. J. Marlowe et al., WANDA-A—One-Dimensional Few Group Diffusion Equation Code for the IBM-704, WAPD-TM-28, November 1956. (Unclassified AEC report.)

56. G. J. Habetler and V. A. Walbran, One-space-dimensional Multigroup for the IBM-650. Part I. Equations. KAPL-1415, 1955; V. A. Walbran, One-space-dimensional multigroup for the IBM-650. Part II. Machine Program, KAPL-1531, 1956. (Unclassified AEC reports.)

57. C. L. Davis, J. M. Bookston, and B. E. Smith, GNU-II—A Multigroup One-dimension-diffusion Program for the IBM-704. GMR-101, General Motors Corp., Detroit, Mich., 1957.

58. O. J. Marlowe and P. A. Ombrellero, CANDLE—A One-dimensional Few Group Depletion Code for the IBM-704, WAPD-TM-53, May 1957. (Unclassified AEC report.)

59. E. L. Wachspress, CURE—A Generalized Two-space-dimension Multigroup Coding for the IBM-704, KAPL-1724, Apr. 30, 1957. (Unclassified AEC report.)

60. G. G. Bilodeau et al., PDQ—An IBM-704 Code to Solve the Two-dimensional Few Group Neutron-diffusion Equations, WAPD-TM-70, August 1957. (Unclassified AEC report.)

61. P. Greebler, TRIXY—A Computer Program for Multigroup Nuclear Reactor Calculations in Three-space Dimensions, KAPL-1549, 1956. (Unclassified AEC report.)

62.* W. H. Zinn and P. Godwin, The Use of Nuclear Energy for Purposes Other Than the Generation of Electricity, A/CONF.15/P/1831.

63. R. M. Ball et al., Critical Experiments for the N. S. Savannah Core, meeting of the American Nuclear Society, Detroit, Mich., December 1958.

64.* P. Blomberg, E. Hellstrand, and S. Horner, Measurements and Calculations of the Temperature Coefficient of the Effective Resonance Integral in Uranium Metal and Oxide, A/CONF.15/P/150.

65. E. Hellstrand, Measurements of the Effective Resonance Integral in Uranium Metal and Oxide in Different Geometries, *Journal of Applied Physics*, 28(12): 1493-1502 (1957).

66. G. W. Rodeback, Temperature Coefficients of Uranium and Thorium Resonance Integrals, NAA-SR-1641, 1956. (Unclassified AEC report.)

67. R. M. Pearce and D. H. Walker, A Direct Measurement of the Uranium Metal Temperature Coefficient of Reactivity, *Nuclear Science and Engineering*, 2: 24 (1957).

68. M. V. Davis, Resonance Capture of Neutrons by Uranium Cylinders, HW-37766, 1955. (Unclassified AEC report.)

69. D. J. Behrens, The Effect of Holes in a Reacting Material on the Passage of Neutrons, *Proceedings of Physical Society (London)*, 62A: 607 (1949).

70.* A. P. Schmitt et al., Natural Uranium-Graphite System, A/CONF.15/P/1191.

71. L. Seren, An Experiment Test of Behrens' Theory, Measurement of Anisotropic Diffusion Lengths in Graphic Containing 25% Void, meeting of the American Nuclear Society, Detroit, Mich., December 1958, Paper 3.6.

72.* B. Cutts et al., Graphite Moderated Thermal Reactor Calculations for the Calder Hall Reactors, A/CONF.15/P/15.

73.* H. Rose, W. A. Cooper, and R. B. Tattersall, The Use of the Pile Oscillator in Thermal Reactor Problems, A/CONF.15/P/14.

74. C. H. Westcott, Effective Cross Section Values for Well-moderated Thermal Reactor Spectra, CRRP-680, 1957. (Unclassified Canadian report.)

75. C. H. Westcott, Effective Cross Section Values for Well-moderated Thermal Reactor Spectra, CRRP-787, (Rev. II, 1958), Aug. 1, 1958. (Unclassified Canadian report.)

76. K. L. Aitken and F. W. Cornish; cited in reference 73.

77. R. L. Macklin and H. S. Pomerance, Resonance Capture Integrals, *Proceedings of the International Conference on the Peaceful Uses of Atomic Energy, Geneva, 1955*, 5: 96-101 (1956).

78. P. W. Mummery, Proceedings of the Brookhaven Conference on Resonance Absorption of Neutrons in Nuclear Reactors, BNL-433, pp. 51-53, 1956. (Unclassified AEC report.)

79. J. A. Harvey and J. E. Sanders, Summary of Data on the Cross Sections and Neutron Yields of U^{233}, U^{235}, and Pu^{239}, in "Progress in Nuclear Energy," Vol. 1, pp. 1-54, Pergamon Press, Inc., New York, 1956.

80. A. M. Weinberg, Highlights of Geneva Conference:

Reactor Physics, meeting of the American Nuclear Society, Detroit, Mich., December 1958.

81. P. A. Egelstaff, K. W. Morton, and J. E. Sanders, A Discussion of Thermal Neutron Data, NRDC-84. (Unclassified British report.)
82. C. G. Campbell and R. G. Freemantle, Effective Cross-Section Data for Thermal Reactor Calculations, AERE-RP/R2031. (Unclassified British report.)
83.* D. S. Craig et al., Long Irradiation of Natural Uranium, A/CONF.15/P/205.
84. D. C. Hurst et al., NRX Rod No. 683, Analysis of Irradiated Uranium and Estimation of Effective Cross Sections, CRR-622(Rev.), May 1957. (Unclassified Canadian report.)
5. I. W. Richardson et al., Reactor Physics of H_2O-Moderated Power Reactors, ASAE-S-7, Feb. 1, 1958. (Unclassified AEC report.)

*Second United Nations International Conference on the Peaceful Uses of Atomic Energy, Geneva, September 1958. (Available from the Office of Technical Services, Dept. of Commerce, Washington 25, D. C.)

Heat Transfer and Thermal Cycles for Gas-cooled Systems

The gas-cooled power reactor, which for a number of years saw little development in the United States as a central-station type, is now becoming an important part of the U. S. program. The heat-transfer characteristics of gaseous coolants are quite different from those of liquids, and the interrelationships among the thermal variables to determine an optimum plant design are rather different from those which apply for liquid-cooled reactors. Consequently, studies which treat the relationships of the thermal variables to each other and to other aspects of the plant design are particularly pertinent at this stage of the gas reactor program in the United States. The papers reviewed below reflect mainly the results of the British investigations in these areas.

Probably the outstanding features of gas-cooled systems as distinguished from those cooled by liquids are the lower heat-transfer coefficients, the large coolant volumes required, and the rather large amounts of power required to circulate the gas coolant. The power consumed in circulating the coolant in a gas-cooled reactor plant is typically of the order of 8 per cent of the plant's gross electric output. It is therefore very important to minimize the pressure drop in the gas-coolant circuit.

A large part of the power consumption connected with coolant circulation occurs in the steam generators of a gas-cooled power reactor system. Reference 1 points out that actually two major consumption items occur in the steam generator. The first is the gas side pumping power associated with the gas pressure drop through the steam generator heat-transfer surface. The second is the power loss implied by the existence of finite temperature differences between the gas and water sides. This makes the transfer of heat irreversible and therefore causes a loss of theoretically available power. The two power losses can be summed to obtain the total power loss incurred by a steam generator.

The power loss due to the temperature difference can be increased or decreased by changing the amount of heat-transfer surface. The change in heat-transfer surface can be obtained by changing either the heat-exchanger face area or its length. In either case. the gas pressure drop, and therefore the power loss due to pumping power will be affected. Reference 1 points out that there is an optimum balance between the heat-transfer performance, as reflected in the gas-steam temperature difference, and the pressure drop for the steam generators of a gas-cooled reactor.

The reference also presents a method of evaluating and correlating these interrelated parameters for any given type of heat-transfer surface configuration. The graphically illustrated results presented are based on the circumferentially finned steel Integron tube used in the British Bradwell power station. They are not intended to cover heat-transfer tube dimensions or arrangements differing greatly from that particular type. Qualitatively similar results could, however, be obtained for other configurations.

The graphical results presented in the reference include only the thermodynamic considerations. No consideration is given to the capital investment costs involved, but importance of this factor is acknowledged. The effect of taking the cost of heat-transfer surface into account would be to shift the optimum parameters toward less heat-transfer surface.

A more complex problem in gas-cooled reactor design is the optimization of the reactor coolant gas conditions and the steam cycle conditions for lowest power cost.

Reference 2 presents a study that evaluates the thermodynamic optimum steam cycles and their efficiencies for gas-cooled reactors as the gas outlet temperature is increased. The range of gas outlet temperatures considered is from the 662°F of Calder Hall to 1110°F. The types of steam cycles considered are single pressure,

dual pressure, and super critical, each with and without reheat. The analysis is based on reactors of the Calder Hall type.

Table III-1 shows steam cycles and operating conditions that were found to be optimum as the attainable outlet coolant temperature was assumed to increase. It is to be noted that the single pressure cycle is not indicated to be optimum at any point over the temperature range considered. The dual-pressure cycle showed the highest gains over the single-pressure cycle when the coolant temperature leaving the steam raising plant was low. The relative positions of the two cycles would no doubt be changed if the increased cost of equipment for the dual-pressure cycle, especially that of the heat exchangers, were taken into account.

inlet temperature can be increased to the point that feed-heating can be used to great advantage. Much of the potential improvement in cycle efficiency with increased coolant outlet temperature stems from the fact that the coolant inlet temperature can be raised as well. The restriction on inlet temperature for a given outlet temperature arises from pumping-power considerations and from the circumstance that some specified amount of power must be removed from the reactor. In the analysis of reference 2 the pumping power is held constant at 10 per cent of the net power output of the plant, and the reactor power density is evidently held constant, at an unspecified value.

The report apparently evaluates cycles entirely on a thermodynamic basis. Since no men-

Table III-1 ADVANCED REACTOR STEAM CYCLE DATA

Coolant outlet temperature, °C	350	400	450	500	550	600
Coolant outlet temperature, (°F)	(660)	(750)	(840)	(930)	(1,020)	(1,110)
Coolant inlet temperature,* °C	177	222	260	294	320	343
Coolant inlet temperature, (°F)	(350)	(430)	(500)	(560)	(610)	(650)
Type of steam cycle	Dual pressure		Dual pressure with reheat		Super-critical with reheat	
H. P. steam pressure, psi	600	920	2,000	2,800	3,500	5,500
H. P. steam temperature, °C	640	730	820	910	1,000	1,090
H. P. steam temperature, (°F)	(337)	(387)	(438)	(487)	(537)	(590)
L. P. steam pressure, psi	150	230	500	860		
L. P. steam temperature, °F	620	710	820	910		
L. P. steam temperature, (°C)	(327)	(376)	(438)	(487)		
Reheat pressure, psi					1,200	1,800
Reheat temperature, °F					1,000	1,090
Reheat temperature, (°C)					(537)	(590)
Proportion of h.p. steam, %	60	64	67	79	100	100
Feed water temperature, °F	200	375	455	515	520	580
Feed water temperature, (°C)	(93)	(191)	(235)	(268)	(272)	(305)
Turbine cycle efficiency, %	28.2	33.5	38.0	41.0	43.5	45.0
Turbine exhaust moisture, %	13.5	14.0	10.5	11.5	11.5	12.0
Station over-all efficiency, %	25	30	34	37	39	40.5
Efficiency with single-pressure steam cycle, %	23.0	28.0	31.5	34.5	36.5	37.5
Corresponding turbine exhaust moisture, %	11.0	12.5	14.5	†	†	†

*Coolant temperature at inlet to circulators.
†Excessive moisture content.

A large increase in the attainable steam pressure and a correspondingly attractive improvement in the over-all thermal efficiency are seen to result from relatively modest advances in reactor coolant outlet temperature. When coolant outlet temperatures are limited to about 750°F, the effective use of feed-heating is not possible since it would be done at the expense of steam pressure. As the coolant outlet temperature is increased above this value, however, the coolant

tion is made of capital investment costs, the method of selecting the optimum cycle is not clear. It appears that the optimum cycles selected are very near those which give maximum over-all plant efficiency with an acceptable turbine exhaust moisture. The report does point out that in the final selection of optimum cycle conditions, practical and economic considerations must supervene and that economic considerations lead to selection of coolant return tem-

peratures (and hence efficiencies) lower than the indicated thermodynamic optimum. As an example of this, the thermodynamic optimum indicated by the results of the report would correspond to a coolant temperature at the exit of the steam raising plant of 370 to 400°F for the 662°F reactor exit temperature of Calder Hall. In the feasibility study for Calder Hall, however, the coolant temperature leaving the steam raising plant was selected at 350°F.

In the foregoing discussion no details of the heat transfer within the reactor were considered. The internal heat transfer is of great importance, for it affects the total power attainable from a given reactor, the pumping power, and the attainable outlet temperature. Extended heat-transfer surfaces are often used in gas-cooled reactors to obtain higher heat fluxes from the fuel for a given temperature difference between fuel and coolant. A discussion of earlier data on the Calder Hall transverse fins was given in a previous issue of this review.[3] The British have also performed experimental work on other configurations of extended surfaces. Reference 4 presents test results on a configuration consisting of multistart helical fins intersected by four longitudinal splitters. Correlations of heat transfer and friction factor were made relative to the number of starts and the lead of the helix over a range of Reynolds number.

The dimensions of the finned tube configuration treated in reference 4, which were constant for all cases considered, were

Outer diameter of fins, in.	2.0
Diameter of fin root, in.	1.25
Number of splitters	4
Thickness of splitters, in.	0.064
Radial clearance between outside of splitters and channel wall, in.	0.050
Finning material	Magnox A-12

The range of variables considered was

Inside diameter of flow channel, in.	3.5 to 4.125
Number of helix starts	30 to 48
Helix leads, in.	12 to 40
Metal to gas temperature difference, °C	50 to 90
Reynolds number	3×10^4 to 7×10^4

Atmospheric air was used as the coolant gas for all tests. Temperature dependent variables were determined by using average thermocouple readings.

The test results obtained show that the following equation predicts the Stanton number and therefore the heat-transfer properties to ±12 per cent within the 95 per cent confidence limits.

$$St = 10^{-5}\left(\frac{8800}{N}+\frac{2500}{L}-44\right) \times \left(\frac{Re\ kg/km}{16}\right)^{-0.34+0.0063\ (L-22)}$$

where N = number of fin starts
L = lead of helix, in.
k_g and k_m = thermal conductivity of gas and metal, respectively

The Stanton number was found to vary about ±10 per cent in a definite sinusoidal pattern along the length of the test section. The friction factor, as calculated from pressure-drop measurements, includes the effect of mixing of the gas by the fins. The following equation was found to correlate the data within ±20 per cent.

$$f = Re^{-0.137}\left(\frac{17.28}{LN}+0.0126\right)$$

Gas velocity profiles were taken over the flow cross sections. These showed local velocities of about 80 per cent of the mean along the tube and fin surfaces and as high as 155 per cent of the mean in the approximate centers of the flow sections. With an increase in flow channel diameter, and constant tube and fin dimensions, it might be expected that the section bounded by the splitters, the fin tips, and the channel wall would rob the gas flow between the fins and thereby significantly reduce the effective heat-transfer coefficient. Comparison of results for different diameters showed, however, that such an effect did not occur over the interesting range of diameters.

The data reported in reference 4 for two different flow channel dimensions are as follows:

C	D_e	N	L	St_s	A_f	V
3.5	0.695	30	18	515	1.0	1.47
4.125	0.932	30	18	509	1.47	1.0

where C = flow channel diameter, in.
D_e = equivalent hydraulic diameter, in.

N = number of fin starts
L = length of helix lead of fins, in.
St_8 = Stanton number for: (Reynolds number)(ratio of gas conductivity/fin conductivity) = 8
A_f = relative flow area
V = relative velocity

The theoretical effect of diameter on the heat-transfer coefficient, h, assuming no by-passing of the flow, should be given by the equation:

Nusselt number =
(constant) (Reynolds)$^{0.8}$ (Prandtl)$^{0.4}$

$$\frac{h_{4.125}}{h_{3.5}} = \left(\frac{V_{4.125}}{V_{3.5}}\right)^{0.8} \times \left(\frac{D_{3.5}}{D_{4.125}}\right)^{0.2} = 0.69$$

If the relative values of h based upon the *measured* values of Stanton number (St_8 above) are compared:

$$\text{Stanton number} = h\left(\frac{1}{C_p\, V\rho}\right)$$

here C, the specific heat, and ρ, the density of the gas, remain constant for the two cases. Then

$$\frac{h_{4.125}}{h_{3.5}} = \frac{509}{518} \times \frac{1}{1.47} = 0.67$$

Thus, for this geometry and flow condition, the calculated ratio of heat-transfer coefficients, using average conditions and the conventional heat-transfer equation, is very close to the measured ratio. It therefore may be said that no robbing of flow effect was observed. The obvious conclusion is that good mixing is provided by the splitters and the helix.

In the previous discussion of the Calder Hall fins in this Review[3] plots were made of Nusselt number vs. Reynolds number and of (Stanton number) (Prandtl number)$^{0.6}$/(½ friction factor) vs. Reynolds number; the latter curve gives the heat-transfer/friction ratio, and is an indication of the price paid in friction pressure drop (and therefore pumping power) for the improved heat transfer provided by the fins. The results of reference 4 can be compared in this respect with the Calder Hall results. If the value of the ratio of k (gas)/k (magnox fins) is taken as about 2.6×10^{-4}, then the St_8 measured for the extended surface configuration tested in reference 4 corresponds to a Reynolds number of 3.09×10^4, and St_{18} corresponds to Re = 6.18×10^4. The corresponding Nusselt numbers are 110 and 170, respectively. When these values are plotted on the previously mentioned graphs* of reference 3, it may be seen that the extended surface configuration of reference 4 gives a performance about equal to that of the "roughened tube."

When heat-transfer tests are made on systems containing extended surface, the direct result is an "effective" heat-transfer surface coefficient. Often the desired result is a "local" or true surface coefficient. Reference 5 presents a method of directly evaluating the "local" coefficient without a trial-and-error solution that is required by the more straightforward procedure. The method presented is an approximate solution that may introduce an error of about 2 per cent. In what is probably the more typical situation of performing design calculations, rather than analyzing test data, the problem discussed by this paper does not occur.

Reference 6 derives the appropriate mathematical equations for use in analogue computer studies of the transient characteristics of a gas-cooled graphite-moderated reactor.

Properties of Gases

Problems involving the properties of gases occur in reactor technology for widely different applications such as gas cooling, energy absorption in containment gases, gas-bonding of fuel and jackets, and hypothetical reactor explosions. Fairly accurate (< 5 per cent error average) calculations for thermal conductivities of gas mixtures can be made, with quite limited pure-gas input data, by using formulas derived in references 7 and 8. These formulas are correlated with experimental data.

Reference 7 is a detailed thesis with new, careful experiments to determine thermal conductivity and viscosity for pure and mixed gases at temperatures up to 540°C. The empirical formula offered by reference 7 fits experimental data a bit more accurately than the quite similar expression of reference 8 which has the advantage of having one less input parameter (that is difficult to determine) and further, is derived from rigorous theory with certain approximations to reduce the complexity of calculations. Obvious advantages occur for use of this formu-

*Figs. 4 and 5, pp. 9 and 10, of reference 3.

lation when high-temperature problems are considered for gas mixtures in connection with detonations and shock waves.

When mixtures of fission gases (xenon and krypton) with helium are considered, the large differences in atomic weight cause marked deviations from the simple mixing law. A helium "bond gas," used to improve heat transfer from a fuel element like UO_2 to its metallic jacket, will have a slow dilution from krypton and xenon with exposure since some fission gases escape the solid fuel and mix with the helium. The relatively low thermal conductivities of xenon and krypton seriously impair the conductivity of the gas bond, and it is important to allow for this effect in the fuel element design. The formulas of references 7 and 8 are applicable and may be found useful for this case.

Reference 9 concerns essentially the same problems faced by references 7 and 8 but for considerably higher temperatures, 1000°K to 15,000°K, which are beyond the present realm of laboratory tests. The basic theory of molecular interactions is defined using experimental results from molecular-beam-scattering experiments. The results offer an approach only, since effects of excitation, dissociation, and ionization are not considered.

References

1.* F. Carr, C. Rounthwaite, and P. A. Young, Evaluation of Finned Tubes for Steam Generators in Gas Cooled Power Reactor Systems, A/CONF.15/P/2327.

2.* W. R. Wooton, A. J. Taylor, and N. G. Worley, Steam Cycles for Gas-cooled Reactors, A/CONF. 15/P/273.

3. *Power Reactor Technology*, 1(1): (December 1957). (Available from Superintendent of Documents, U. S. Government Printing Office, Washington 25, D. C.)

4.* D. F. Hughes and M. R. Slack, A Correlation of Heat Transfer for Finned Fuel Elements for Carbon Dioxide Cooled Reactors, A/CONF.15/P/38.

5. G. M. Dusinberre, Effective and Local Surface Coefficients in Fin Systems, *Transactions of the American Society of Mechanical Engineers*, 80(7): 1596-1597 (October 1958).

6.* T. J. O'Neill, The Derivation of Reactor Heat Transfer Transient Equations for Gas-cooled Graphite Moderated Thermal Reactors, A/CONF. 15/P/21.

7. Henry Cheung, Thermal Conductivity and Viscosity of Gas Mixtures, UCRL-8230, April 1958. (Unclassified AEC report.)

8. E. A. Mason and S. C. Saxena, Approximate Formula for the Thermal Conductivity of Gas Mixtures, *The Physics of Fluids*, 1(5): 361 (September-October 1958).

9. I. Amdur and E. A. Mason, Properties of Gases at Very High Temperatures, *The Physics of Fluids*, 1(5): 370 (September-October 1958).

*Second United Nations International Conference on the Peaceful Uses of Atomic Energy, Geneva, September 1958. (Available from the Office of Technical Services, Dept. of Commerce, Washington 25, D. C.)

The inclusion of a burnable poison in reactors has been considered for some time as a means of extending the reactivity lifetime and decreasing the number of conventional control rods required. Burnable poison was first used in the BORAX-III reactor,[1] in 1955. In reactors having conversion ratios less than unity, the burn-up of fissionable material gradually decreases the available reactivity in the reactor during the life of the fuel loading, until eventually the available reactivity is not sufficient for operation of the reactor. The length of time required to reach this point may be adjusted by the amount of initial excess reactivity incorporated into the fuel loading. However, in the early stages of the reactivity lifetime, this excess reactivity must be controlled by the presence of control rods or other control means. A burnable poison may be used as one of these means of control. It consists of some neutron-absorbing isotope which, upon the absorption of neutrons, is converted to an isotope of low absorption. For this purpose materials are chosen of such cross sections that the rate of burn-up of the absorbing isotope approximately compensates for the rate of reactivity loss by fuel burn-up. Two advantages which result from the use of a burnable poison for the added control are (1) a smaller flux distortion than in the case of control rods and (2) a saving in the number of control rods required and a saving in space both in the control rod drive area and in the reactor core.

The usual application of burnable poisons is in highly enriched reactors containing negligible quantities of fertile materials. For thermal reactors of this type, if the fission-product poisoning and the change in neutron leakage with diffusion length are neglected, the relation between reactivity change and fuel burn-up is approximately

$$\frac{dk_{eff}}{k_{eff}} = \frac{dM}{M}\left(1 - \frac{k}{\eta}\right)$$

where dM/M is the fractional change in the mass of fissionable isotope in the reactor, k is the infinite multiplication constant, and η is the number of neutrons produced per neutron absorbed in the fissionable isotope. The range of $(1 - k/\eta)$ for practical reactors is perhaps from about 0.1 (k = 1.86) to about 0.5 (k = 1.04), and in many fully enriched reactors it is between 0.3 and 0.4. It is clear that for most such reactors the change in reactivity with fuel burn-up is rapid, and if, for example, it is desired to burn 50 per cent of the fuel in the core, the corresponding reactivity change will be very large unless some scheme such as burnable poisons is used.

Ideally there is a certain effective cross section for the burnable poison which will cause it to burn out at a rate which very nearly compensates for the reactivity loss due to fuel burn-up and fission-product poisoning. Furthermore, it is desirable that the burnable poison be completely consumed so as to minimize the total fuel inventory required. That this ideal behavior cannot be expected from a single uniformly distributed burnable poison is apparent from rather simple considerations. The equation for k_{eff} of a uniform, thermal, nonconverting reactor can be written as

$$k_{eff} = \frac{\eta}{1 + M^2B^2} \frac{1}{1 + (\Sigma_r/\Sigma_{25})}$$

where Σ_{25} is the macroscopic absorption cross section of the fissionable isotope and Σ_r is the macroscopic absorption cross section of all other materials in the reactor (including the burnable poison). If again fission-product poisoning and the change in neutron leakage (i.e., the change in M^2B^2) are neglected, then k_{eff} would remain constant with fuel burn-up provided the ratio Σ_r/Σ_{25} remained constant. If the burnable poison were the only absorber present other than the fissionable isotope, the ratio would remain constant if (and only if) the *microscopic* absorption cross section of the burnable poison were equal to that of the fissionable isotope. However, the poison would not be completely burned out until the fissionable isotope was also completely burned out. In

practice, Σ_r is made up of other absorptions besides that of the burnable poison. For this case, if one can choose any desired microscopic cross section for the burnable poison, one can make the ratio Σ_r/Σ_{25} equal to its initial value at one chosen degree of fuel burn-up, but at no more than one. To do this, the fractional rate of poison burn-up must be chosen to be higher than that of the fuel by an appropriate amount (that is to say, the microscopic absorption cross section of the poison must be larger than that of the fuel). Obviously the initial rate of burnout of the poison will then be too high. Thus the characteristic behavior of reactivity when a single, uniformly distributed burnable poison is used is an initial increase with fuel burn-up, followed by a decrease which eventually returns the reactivity to its initial value, followed by a rather rapid reactivity loss with further burn-up.

Numerous and more complicated schemes have been devised to circumvent the difficulties indicated above. The analysis of these schemes is complex, and the flux perturbations caused by control rods and by the burnable poison itself, as well as the changing neutron spectrum, complicate further the calculations involved in determining the optimum poison concentration and configuration. Some of the burnable poison schemes and the methods of calculation are given in references 2 and 3.

The most commonly considered material for a burnable poison is boron, although dysprosium has also been studied. In epithermal reactors, cadmium shows some promise, although the results are probably quite sensitive to the reactor spectrum. Both boron and dysprosium have thermal absorption cross sections considerably greater than that of U^{235}. The effective cross section may be adjusted, however, by taking advantage of the phenomenon of self-shielding in lumped poison rods. With heavy self-shielding, the effectiveness of the poison does not change with burn-up during the early period of irradiation, and during this period the reactivity of the reactor decreases as the U^{235} is burned. Later, after enough of the poison is consumed to reduce the self-shielding, the burnable poison is consumed faster than the fuel, and the reactivity rises to a maximum before again dropping off with further irradiation. Radkowsky[3] has proposed that the minimum mis-match between poison burn-up and fuel burn-up may be obtained by using burnable poison elements of two different self-shielding factors, adjusted so that the reactivity peak of the lightly shielded poison element coincides with the reactivity dip of the heavily shielded poison element.

Little has been written on the applicability of burnable poisons to converter reactors. It would be expected that in most cases they would not be attractive, since their use implies the consumption of neutrons which might better be used for conversion. This reduction of neutron economy is no greater however than would result from the use of control rods for the same purpose, provided the burnable poison is virtually all consumed during the life of the fuel charge. In the case of the U^{238} converter the behavior of the single, uniformly distributed burnable poison appears unattractive because the reactivity peak provided by the burnable poison would seem to coincide with the plutonium reactivity peak. In thorium converters this consideration does not hold, and indeed, it is possible that a high cross-section burnable poison might serve to level out the initial reactivity dip due to the hold-up of potential U^{233} as protactinium. It has been stated that burnable poison is used in the Consolidated Edison thorium converter reactor.[4]

References

1. Andrew W. Kramer, "Boiling Water Reactors," p. 105, Addison-Wesley Publishing Company, 1958.
2.* A. M. Smith and J. Jeffrey, Burnable Poisons in Small Power Reactors, A/CONF.15/P/86.
3.* A. Radkowsky, Theory and Application of Burnable Poisons, A/CONF.15/P/1900.
4.* G. R. Milne, S. M. Stroller, and F. R. Ward, The Consolidated Edison Company of New York Nuclear Electric Generating Station, A/CONF.15/P/1885.

* Second United Nations International Conference on the Peaceful Uses of Atomic Energy, Geneva, September 1958. (Available from the Office of Technical Services, Dept. of Commerce, Washington 25, D. C.)

Neutron-flux Distribution and Attenuation

In a paper presented at the second Geneva conference,[1] Blizard outlines reactor shielding and discusses basic data requirements, facilities for experimental research, attenuation theory, and recent developments in shielding materials. There is a growing need for better neutron cross-section data and for improved methods to determine neutron flux distributions in shields.

Most of the experiments to determine the widely used fast neutron removal cross sections have been performed at the ORNL Lid Tank Shielding Facility (LTSF). The LTSF measurements require large (142 by 167 cm) slabs of the material under test; for some materials these quantities may be expensive. Reference 2 describes an experiment utilizing relatively small samples of material. The experiment was performed at the Brookhaven Shielding Facility with an air-filled aluminum collimator placed above the converter plate and surrounded by water to provide a fairly small diameter source of essentially monodirectional neutrons. The results of this experiment yield "collimated" removal cross sections for hydrogen, lithium, beryllium, boron, carbon, oxygen, fluorine, sodium, aluminum, sulfur, chlorine, titanium, iron, nickel, copper, cadmium, tungsten, lead, and bismuth. These cross sections are significantly larger than the conventional removal cross sections obtained with a sample close to a distributed isotropic source but can be used for an indication of the relative effectiveness of different shield materials. The monodirectional nature of the source used in the experiment prevents use of the results in the usual way in shield design calculations.

Trubey and Chapman[3] have used the ORNL LTSF to obtain removal cross sections for carbon and oxygen when the material is distributed rather than concentrated adjacent to the source plate. The carbon cross section was determined from a comparison of thermal neutron flux measurements in a sugar solution with measurements in plain water. Since the sugar ($C_{12}H_{22}O_{11}$) solution contained almost as much hydrogen and oxygen as plain water and contained them in the same ratio, the effect of the water could be separated and a distributed cross section for carbon obtained. Then by comparing the measurements in oil and water and using the carbon cross section found as described above, the oxygen cross section was determined. Though differences appear between these "distributed" cross sections and the cross sections determined by the usual method, the indicated differences are well within the experimental uncertainties involved and lead to the conclusion that any actual differences are probably small.

Bourgeois et al.[4] present removal cross sections obtained experimentally and theoretically. The majority of the values given are the results of experiments performed at the French NAIADE facility and agree fairly well with previously reported cross sections. The theoretical calculations treated energy-dependent fast neutron removal cross sections for iron, lead, and water.

A British paper[5] presents a method for predicting the spatial distribution of thermal and epithermal neutron fluxes in hydrogen-metal reactor shields. Such calculations are particularly applicable to the prediction of heat production in thermal shields, pressure vessels, and other materials relatively near the reactor core. The three-group model described provides a value of the thermal flux accurate to better than 20 per cent. Empirical parameters are required for application of the method to complex multilayered systems. The experiments were performed at the Harwell shielding reactor, LIDO, which consists of a core of enriched U-Al alloy suspended in a water-filled concrete tank with aluminum-faced cavities at three positions around the tank walls. Large-scale shielding experiments may be constructed outside a cavity and the core may then be moved to within a few centimeters of the inner face of

the cavity. Iron was chosen as the metal in the hydrogen-metal shield, and after empirically deriving the slowing-down lengths in the shield materials, applying these lengths to the three-group model, and comparing the semianalytic results with further experimental measurements, 20 per cent or better accuracy for the thermal flux distribution was found to prevail in shield systems containing from 2.4 to 37.4 cm of iron.

Duncan and Whittum[6] have developed a relatively simple method of determining fast and thermal neutron flux distributions at deep neutron penetrations in hydrogenous shields. The method uses fast neutron removal theory in conjunction with a two-group diffusion model for calculating the thermal neutron flux distribution. It is accurate only in hydrogenous shield regions several diffusion lengths from nonhydrogenous boundaries. The authors note that since the method overestimates the thermal flux in the nonhydrogenous portions of a shield and is simple in comparison with other methods, it may find use in preliminary design studies.

Concretes for Reactor Shielding

The low unit cost of concrete has resulted in its use as shielding for nearly all power reactors where shield thickness and weight are not critical. The "standard" methods have generally been employed to calculate required thicknesses of concrete; i.e., the moments method for gamma-ray attenuation and the removal cross section concept for fast-neutron attenuation. The removal cross-section concept was originally developed for hydrogen-rich shields. It assumes a scatter collision to be equivalent to an absorption. It would be expected to apply only to shields which have a relatively short slowing-down length for first-collided neutrons. Since the validity of the concept thus depends primarily on the slowing-down capability of the shield-contained moderator, its applicability to concrete shields without added hydrogen has been questioned. However, concrete contains a considerable amount of oxygen which by elastic scattering augment the hydrogen moderation.

To determine the actual hydrogen requirements for concrete shielding and to compare measured gamma-ray attenuation to moments-method calculations, Blizard and Miller[7] performed a series of tests on ordinary concrete at the ORNL LTSF. The rather thorough tests show that with no added hydrogen, ordinary concrete with a 7 wt.% water content attenuates the intermediate-energy neutrons considerably more strongly than it does the very fast neutrons, thereby indicating adequate moderation. The conclusion is that in concretes containing at least 7 wt.% water, the shield attenuation rate is characteristic of the very fast neutrons and is adequately described by the removal cross-section method. The measured gamma-ray attenuation was in good agreement with calculated attenuation.

Although the test procedure is not described, reference 4 contains experimental values for removal cross sections of concrete obtained in the French NAIADE device, a facility very similar to the ORNL LTSF. Ordinary and heavy concretes were tested, and the cross sections obtained $\Sigma_R = 0.085$ cm^{-1} to 0.125 cm^{-1} are generally in good agreement with those reported in references 7 and 8. The aggregates utilized in the French concretes result in mixes chemically similar to those used in the United States.[7,8,9]

The measured attenuation in the ORNL Graphite Reactor shield is described in detail by Blosser et al.,[8] and cross plots of the data should furnish interesting information concerning radiation streaming through a cylindrica void in a concrete shield.

The articles reprinted in reference 9 deal principally with selection and proportioning of the constituents of concretes, but also yield the following information: (1) barytes concrete mixed and placed by conventional methods has about twice the compressive strength of prepacked barytes concrete; (2) conventional barytes concrete compares favorably with ordinary concrete when subjected to severe thermal cycle, but prepacked barytes concrete is inferior; and (3) conventional barytes concrete and prepacked barytes concrete exhibit almost twice the thermal coefficient of expansion of ordinary concrete and have relatively very low values of specific heat, thermal conductivity, and diffusivity. Reference 8 indicates that ordinary and barytes-haydite concretes suffer about the same percentage loss in compressive strength when subjected to heat.

Clark[10] has published a compilation of data obtained by a literature survey on the subject of radiation damage to concrete. The only ap-

parent deleterious effect resulting from irradiation is the production of gas by boron-containing cements. For the majority of reactors, it is unlikely that there would be any appreciable change in the properties of the shield due to radiation damage during the operational lifetime. A far more serious problem is overstressing as a result of nuclear and external heating.

References

1.* E. P. Blizard, The Shielding of Nuclear Reactors, A/CONF.15/P/2162.
2. R. D. Schamberger, Effective Removal Cross Section with a Monodirectional Source of Fission Neutrons, WADC-TR-58-266, January 1958. (Unclassified AEC report.)
3. D. K. Trubey and G. T. Chapman, Effective Neutron Removal Cross Sections for Carbon and Oxygen in Continuous Mediums, ORNL-2197, Sept. 19, 1958. (Unclassified AEC report.)
4.* J. Bourgeois et al., Methods and Experimental Coefficients Used in the Computation of Reactor Shielding, A/CONF.15/P/1190.
5.* C. Cooper, J. D. Jones, and C. C. Horton, Some Design Criteria for Hydrogen-Metal Reactor Shields, A/CONF.15/P/84.
6. D. S. Duncan and H. O. Whittum, Jr., Application of Fast Neutron Removal Theory to the Calculation of Thermal Neutron Flux Distributions in Reactor Shields, NAA-SR-2380, July 1, 1958. (Unclassified AEC report.)
7. E. P. Blizard and J. M. Miller, Radiation Attenuation Characteristics of Structural Concrete, ORNL-2193, Aug. 29, 1958. (Unclassified AEC report.)
8. T. V. Blosser et al., A Study of the Nuclear and Physical Properties of the ORNL Graphite Reactor Shield, ORNL-2195, Sept. 8, 1958. (Unclassified AEC report.)
9. Concrete for Radiation Shielding, Compilation No. 1; reprinted from articles appearing in *Journal of the American Concrete Institute*. (Available from American Concrete Institute, P. O. Box 4754, Redford Station, Detroit 19, Mich.)
10. R. G. Clark, Radiation Damage to Concrete, HW-56195, Mar. 31, 1958. (Unclassified AEC report.)

* Second United Nations International Conference on the Peaceful Uses of Atomic Energy, Geneva, September 1958. (Available from the Office of Technical Services, Dept. of Commerce, Washington 25, D. C.)

Electron-beam Vacuum-welding Process

Because of the potential economic and technical advantages of electron-beam welding, this welding technique is being investigated for making fuel-element closures and welding reactor structural materials. At present, the most commonly used welding method for these applications is the inert-gas shielded tungsten-arc technique. A disadvantage of this method is the possible weld contamination from either the electrode materials or impurities in the inert-gas shielding atmosphere. Difficulty is also encountered in the joining of components of dissimilar thickness.

The vacuum-welding technique employs a highly concentrated beam of rapidly moving electrons which locally fuses the parts to be joined. The electrons are emitted by a heated tungsten filament, accelerated through a high electrostatic potential difference, and focused electrostatically to form a "spot" from $\frac{1}{32}$ to $\frac{1}{8}$ in. in diameter at the junction to be welded. The size and penetration of the molten zone are functions of the electric power fed into the electron beam and of the degree of focusing. Welding is done at a pressure of 10^{-3} mm Hg or less. At higher pressures, ionization can occur, resulting in arcing and consequent loss of focusing ability.

The electron-beam welding process is said to possess a number of significant advantages over the customary shielded arc technique. First, the fusion welding of widely differing thicknesses of materials can be done easily. This is accomplished by adjusting the focus of the beam to obtain the desired "spot" diameter and the accelerating potential to give the required penetration.

Hanford[1] has been developing the electron-beam vacuum-welding process to overcome some of the limitations of the inert-gas shielded process. The method was applied to the welding of end caps on Zircaloy-2-, aluminum-, and stainless-steel-clad fuel elements and to other component materials such as copper, gold, nickel, silver, platinum, and uranium.

Hanford[1] has reported that a power input of 20 watts is sufficient to weld foil, whereas up to 1000 watts is used to fuse satisfactorily $\frac{1}{8}$-in.-thick materials. It was also claimed that very low contamination of the material in the weld zone was achieved. Since no electrode is used, contamination of the weld by electrode materials is impossible. Similarly, the high vacuum required by the process reduces impurities in the welding atmosphere to a negligible quantity. The result is a product having more ductility and greater corrosion resistance than can be obtained with the more conventional welding processes. Corrosion tests of electron-beam vacuum-welded Zircaloy-2 fuel cans in 686°F deionized water indicated that corrosion resistance of the weld and heat-affected zone was as good as or better than the parent metal.

Another advantage mentioned in the reference report is the improved mixing of the molten material, to yield a more uniform metallurgical structure in the fused zone. The electron-beam welded specimens are characterized by a homogeneous acicular grain structure with a complete absence of gas pockets or "pipes" of foreign materials. Tests are reported[1] to indicate that the properties of the fused and heat-affected zones are superior to those of the parent material.

The electron-beam welding process has been used successfully by the French.[2] Aluminum-clad fuel elements, for the Saclay EL-3 reactor, had 2-mm-thick end caps welded to 1-mm-thick cans by this method. Stainless steel, zirconium, beryllium, aluminum, molybdenum, uranium, and magnesium were also welded using this technique. Some difficulty was encountered by the French with the welding of magnesium because the magnesium vapor formed during the fusing led to ionization and arcing in the vacuum

chamber. This difficulty was overcome by using a pulsating source of electrons and proper control of the motion of the piece being welded. A large size electron-beam vacuum-welding machine has been constructed in France to weld large zirconium assemblies. This machine was used to weld the tank of "Proserpine," a plutonium salt-fueled homogeneous reactor.[2]

Bettis Plant is also constructing an electron-beam welding apparatus to be used to weld Zircaloy-2 components for the second core of the Shippingport Pressurized Water Reactor.[3]

Operational costs (not including labor) are said to be substantially lower for the electron-beam process than for the shielded-arc process. Because the electron-beam process must be virtually completely automatic, the initial cost of equipment may be high compared to that for the tungsten-arc method. However, for the mass production of fuel elements a high degree of mechanization is desirable, in any case, and the potentially good controllability of the electron-beam process along with its other advantages may make it the economically preferable one.

Electrocladding of Fuel Elements

Aluminum-clad uranium-metal fuel elements have been used extensively in reactors. Most of these elements have been made up of uranium-metal fuel, AlSi bonded to aluminum cans[4] or have been U-Al alloys or dispersions roll clad with aluminum. Atomics International[5] has recently reported on their development of an electrocladding technique of canning fuel elements. The method involves the use of a continuously regenerative, nonaqueous, aluminum electrodeposition process. An intermediate nickel layer on the uranium metal is used to promote bonding without formation of a brittle intermetallic bond zone. It was reported by Atomics International that dense, adherent claddings of aluminum up to 25-mil thickness were produced on nickel-plated cores by electrodeposition; metallurgical bonding of the electrocladdings was obtained by a thermopneumatic process.

The production of an integral clad by this method appears to be a distinct advantage over methods requiring end-cap welding, particularly where complicated fuel-element shapes are required such as tubular or twisted ribbon elements.

Because the scope of work on this project was limited, no economic comparison of the fabrication methods can be made.

Lead Bonding of Fuel Elements

In most proposed power reactors employing oxide fuel, the oxide is bonded to the fuel canning material by filling the annular gap with helium. Close tolerances or swaging techniques are therefore required to obtain a very small gap and thereby maintain a small temperature drop across the helium gap. In addition to this, released fission product gases mix with the helium and cause a drop in the thermal conductivity of the mixture, thereby resulting in a higher temperature drop and an increase in the central temperature of the fuel material for the same operating heat flux.

A possible substitute for the helium bond is a lead (Pb) bond which has a relatively high thermal conductivity. This has been done in the aluminum canned ThO_2-UO_2, BORAX-IV elements. However, most of the power reactors being designed use Zircaloy-2 or stainless steel for the oxide fuel can and the compatibility of Pb with these materials is questionable.

Argonne National Laboratory[6] has recently reported preliminary data on the reactions of Pb with ThO_2-UO_2, stainless steel, and Zircaloy-2 at temperatures of 600 and 800°C. Metallographic examination of the reaction zones of the specimens held at these temperatures for 60 days showed: (1) no reaction between Pb and ThO_2-UO_2 or between Pb and stainless steel at temperatures of 600 and 800°C; and (2) no reaction between Pb and Zircaloy-2 at 600°C and some reaction between Pb and Zircaloy-2 at 800°C.

It would appear that, in water type reactors where the bonding layer would probably be less than 350°C, a Pb or possibly a Pb alloy bond for oxide type fuels may be feasible.

References

1. W. L. Wyman and W. I. Steinkamp, Electron Beam Vacuum Welding—Development of Process, HW-55667, Apr. 8, 1958. (Unclassified AEC report.)
2. J. Briola, Automatic Welding of Fuel Elements, Second United Nations International Conference on the Peaceful Uses of Atomic Energy, Geneva,

September 1958, A/CONF.15/P/1161. (Available from the Office of Technical Services, Dept. of Commerce, Washington 25, D. C.)
3. Pressurized Water Reactor (PWR) Project Technical Progress Report for the Period June 24, 1958 to August 23, 1958, WAPD-MRP-75. (Unclassified AEC report.)
4. *Power Reactor Technology*, 1(2): 30 (February 1958). (Available from the Superintendent of Documents, U. S. Government Printing Office, Washington 25, D. C.)
5. G. V. Alm and M. H. Binstock, Aluminum-electrocladding Studies for Proposed OMR Fuel Elements, NAA-SR-2704, Oct. 1, 1958. (Unclassified AEC report.)
6. Metallurgy Division Quarterly Report for April, May, and June 1957, ANL-5790, July 1958. (Unclassified AEC report.)

Graphite

High-purity graphite is used extensively in reactors because of its low thermal-neutron absorption cross section, its relatively high-moderating power, and its good high-temperature properties. These properties, along with its relatively low cost and ease of machining, make it attractive in many applications as a combined moderator and structural material. A detailed review of the properties and irradiation behavior of reactor-grade graphite can be found in references 1 through 12. A brief review, containing some of the more important and recent data on graphite, follows.

Thermal Neutron Absorption Cross Section and Density

Because of the importance of graphite as a moderator, a large effort has been made to remove all impurities in the production of reactor-grade graphite and thereby reduce its absorption cross section to a minimum. Commercial purified graphite is produced in the United States, having a density of ~1.68 g/cm^3 and an absorption cross section of ~0.0037 barn. In a 1958 Geneva conference paper,[13] the French reported their best production graphite has a cross section of ~0.0038 and a density of 1.68 g/cm^3.

These results compare favorably with the value for the absorption cross section of C^{12} of 0.0033 ± 0.00015 barn (2200 meters per second) established by Hennig[14] and the cross section of highly purified graphite of 0.0035 ± 0.0003 barn (2200 meters per second) reported by Muehlhause.[14]

Density

The theoretical density of graphite has been measured at 2.27 g/cm^3. However, reactor-grade bulk densities of only ~1.68 g/cm^3 have been produced in large quantities. A special "double-extrusion" technique reported by the French[13] increased the density of the graphite to ~1.76 g/cm^3. This value is still much lower than the theoretical density, and voids amounting to 20 to 30 per cent of the volume are included in the graphite. These voids consist largely of interconnected micron-size holes which make the graphite permeable to gases and some liquids.

Compatibility of Reactor Coolants with Graphite

Although inert to most materials, graphite at high temperature is subject to oxidation. The large porosity presents a large surface area for oxidation, and consideration must be given to this possibility if oxidizing gases, such as air or CO_2, are used as coolants in contact with graphite. Air will oxidize graphite at relatively low temperatures, and the prime emphasis has been placed on the use of CO_2 and helium as gaseous coolants. Helium, being inert, can be used to very high temperatures before the impurity content of it presents a problem. Carbon dioxide, which is being used in the Calder Hall type reactors, apparently must be used at temperatures below 1000°F to prevent serious graphite oxidation. A recent Geneva paper[15] indicated that the oxidation losses of graphite from the Calder Hall reactors will amount to 0.1 per cent per year. This paper also reviewed some of the studies made by the British on the interaction of moderator graphite and the CO_2 coolant in a radiation field. Under in-pile conditions it was reported that CO_2 and graphite reactions definitely indicated that irradiated CO_2 reacted more rapidly with graphite than non-irradiated CO_2, the rate of reaction being nearly independent of temperature but varying almost linearly with radiation intensity. Three techniques were presented which can be used to inhibit these reactions: (1) Gas phase cracking of hydrocarbons to produce a resistant coating on the graphite; (2) Impregnation with phosphorous compounds; and (3) Deposition of a SiC coating.

Studies have also been conducted in the United States on coating of graphite with NbC, TaC, and

ZrC to permit the use of graphite in reactors operating at high temperature in corrosive atmospheres.[16,17] These coatings are applied by a metallic vapor deposition technique in which the rate of coating is controlled by the diffusion of carbon through the carbide. Sound, adherent uniform coatings were produced which withstood repeated heating and cooling. Extensive thermal cycling tests were not conducted.

General Properties

The properties of unirradiated graphite have been adequately covered in the literature (references 1 through 7) and are not reviewed here. However, further data on the unirradiated properties of graphite at high temperatures (>2000°F)[18] and at very low temperatures (as low as 4°K)[19] have also been reported in the references noted.

Irradiation Behavior

Of major interest to the reactor designer is the effect of irradiation on the properties of graphite. Much information of this type was covered in the 1955 Geneva conference for an irradiation temperature of 30°C and at relatively low exposures.[8,9] In a paper presented at the 1958 Geneva conference further data were presented on the long term irradiation effects at 30°C and at higher temperatures.[20]

In general, the major effects of irradiation on graphite were:

Thermal conductivity:	Markedly decreased
Electrical conductivity:	Markedly decreased
Mechanical strength:	Markedly increased
Stored energy:	Increased
Hardness:	Increased
Dimensional changes:	Normally expands

Typical changes in some of the properties of graphite irradiated for various exposures are shown in Table VII-1.

Above the 5000 Mwd/adjacent ton exposure at 30°C, saturation of irradiation damage effects has been reached, and the annealing of defects is almost as rapid as their rate of production.

Irradiation behavior tests of graphite at higher temperatures has indicated that at temperatures in the 750 to 930°F range the irradiation growth usually associated with graphite can change to a shrinkage with increased exposure. A plot of the test data showed a maximum volume change of approximately + 0.04 per cent at an exposure of ~400 Mwd/adjacent ton followed by a volume decrease with higher burn-up which reached a volume change of approximately −0.2 per cent at 4000 Mwd/adjacent ton. At 4000 Mwd/adjacent ton the rate of change of length parallel to the extrusion direction was ~−0.025 per cent ΔL/1000 Mwd/adjacent ton, and the rate of change of length perpendicular to the extrusion direction was ~−0.015 per cent ΔL/1000 Mwd/adjacent ton.

This effect was also noted in some fundamental studies on graphite which were made to

Table VII-1 PROPERTY CHANGES IN CSF GRAPHITE AT 30°C

(Data taken reference 20)

Symbol	Property	Orientation	Exposure (Mwd/at)* 0	1000	2000	3000	4000	5000	6000
C_0	Crystal layer spacing, A		6.71	7.16	7.48	7.65	7.73	7.78	7.78
L_c	Apparent crystallite size in C_0 direction, A		500	275	125	75	50	25	25
K	Thermal conductivity at 25°C, cal/cm-sec-°C	Perpendicular	0.26	0.0082	0.0066	0.0063	0.0063	0.0062	
		Parallel	0.40	0.0104	0.0078	0.0073	0.0071	0.0070	
SE	Total stored energy, cal/g		0	285	435	550	610	630	
	Total stored energy remaining after a 3 hr anneal at 1000°C, cal/g		0	60	160	250	300	330	

* Exposures are given in terms of megawatt days per adjacent ton. This unit is defined as the amount of reactor radiation received by the sample during the time required for the ton of uranium adjacent to the sample to generate one megawatt-day of fission energy. One Mwd/at is equivalent to approximately 3.9×10^{17} nvt thermal or 6.5×10^{17} nvt total.

determine the relation between internal structure and dimensional stability.[21,22] The results of the studies indicated that the net dimensional change obtained at a given irradiation temperature is dependent on two competing effects: (1) crystal expansion and (2) shrinkage of intercrystalline voids. In tests conducted at temperatures of 660 to 850°F, it was noted that the rate of crystal expansion was reduced under irradiation, and shrinkage of intercrystalline voids caused a net contraction of bulk graphite. In the irradiation experiments reported in reference 20, graphite pore size distribution showed a change from a peak at a pore radius of 200 A for zero exposure and 750 to 930°F to a peak at ~120 A for 4500 Mwd/adjacent ton, indicating a shrinkage of the intercrystalline voids. Preliminary data reported[20] on the effect of irradiation on graphite operating at temperatures above 1000°F show: some increase in crystallite damage; very little further increase in the contraction rate at 1380°F; a greater contraction rate at ~1800°F; and a decrease in the stored energy.

A radiation damage effect of considerable importance in low-temperature reactors is the energy storage effect. This phenomenon is due to the strain energy caused by distortion of the graphite crystals under irradiation. This energy will appear as heat when the irradiated graphite is heated above its irradiation temperature during annealing of the graphite. Typical annealing spectra curves, obtained by Woods et al.[8] by raising the graphite temperature at a constant rate and measuring the heat energy produced, showed a thermal energy release with the peak release occurring at an annealing temperature of ~400°F. Thus, if low-temperature (<200°F) irradiated graphite is raised rapidly to this temperature, self heating can occur. The storage of energy is a function of the irradiation temperature, and the peak energy release at ~400°F disappears with irradiation temperatures much above 250°F.

The effect of the spontaneous energy release was presented in reference 8, where it was calculated that a specimen irradiated at 30°C to exposure of ~5000 Mwd/adjacent ton and heated to about 200 to 450°F, could achieve a spontaneous increase in temperature to approximately 1800°F.

The Windscale accident occurred during a scheduled heating of the reactor graphite for the release of stored energy. It should be noted that the safe release of stored energy can be accomplished with proper precautions. An account of the energy release program carried out on the BEPO reactor on Mar. 14 and 15, 1958, is covered in detail in a 1958 Geneva conference paper.[23]

Other studies on the effects of irradiation on the properties of graphite are covered in a series of papers presented in BNL-489.[14] Of particular interest was a paper on the effect of fission fragment damage to graphite. Such damage can occur when the reactor fuel consists of a dispersion of UO_2 in graphite (Kernohan, reference 14). Tests conducted with graphite–5 wt.% UO_2 specimens containing UO_2 particles of four different particle sizes indicated that at low irradiation temperatures and exposures (30 and 88°C at 0.1 per cent U atom burn-up) the specimen with the largest particle size (586 μ) suffered the least damage. The amount of damage appeared to be inversely proportional to the diameter of the UO_2 particle. Both conventional and fission fragment damage was noted in all specimens, but the fission fragment damage could not be annealed out.

Zirconium and Zirconium Alloys

Because of the low thermal neutron absorption cross section and relatively good mechanical properties of zirconium and its alloys, this material is of interest for various reactor design applications. One of the most important properties which determine whether use can be made of zirconium or its alloys is their compatibility with the coolant. Recent data on the corrosion of zirconium and zirconium alloys in water, steam, and gas environments are reviewed below.

Compatibility in 600°F Water

In general, zirconium and especially the Zircaloy-2 alloy have shown good corrosion resistance in 600°F water. Battelle Memorial Institute,[24] in a brief review of progress in zirconium technology reported corrosion rates for zirconium and Zircaloy-2 as shown in Table VII-2.

Compatibility in 900°F Steam

Zirconium and its alloys are known to have much poorer corrosion resistance in steam than in water at high temperatures. In an

Table VII-2 CORROSION RATES IN WATER AT 600°F

	Avg. weight gain, $mg/dm^2/mo$	Avg. penetration rate,* mils/yr
	Pre-breakaway	
Zirconium	4.2	0.088
Zircaloy-2	5.4	0.113
	Post-breakaway†	
Zirconium	100	2.09
Zircaloy-2	7.0	0.146

* The average penetration rate is calculated on the basis of penetration of the original metal under uniform corrosion conditions over the entire specimen surface due to conversion of zirconium to ZrO_2.

† Occurs after many thousands of hours exposure to 600°F water.

investigation of the problems involved in the development of a zirconium base alloy which would be corrosion-resistant in superheated steam, Nuclear Metals, Inc. (NMI) has made a number of experiments with zirconium and zirconium alloys exposed to 900°F, 1500 psi, superheated steam.[25] The results of these experiments showed that zirconium and annealed samples of Zircaloy-2 and Zircaloy-3 undergo flaking of the oxide within one day of exposure to the 900°F steam. The tin content of the Zircaloy alloys was reported to be very detrimental to the corrosion resistance to steam. Alloys of zirconium containing a minimum of 0.2 wt.% nickel, or ~1 wt.% chromium or ~2 to 3 wt.% iron were tested by NMI and found to have better corrosion resistance than Zircaloy-2; flaking in the 900°F steam environment did not occur for approximately 40 to 60 days. In all of the alloys tested, spalling or flaking occurred at a corrosion product weight gain of approximately 120 to 160 mg/dm^2. These alloys still do not represent usable materials in a superheated steam atmosphere although they are considerably better than pure zirconium, Zircaloy-2, or Zircaloy-3.

Compatibility with a He-CO_2 Gas Mixture

In a study of the effect of reactor atmosphere on zirconium and zirconium alloys Hanford[26] has reported on the in-reactor corrosion rates of zirconium and Zircaloy-2 exposed to a 50 vol.% helium – 50 vol.% CO_2 atmosphere (Table VII-3) at a weighted average temperature of 430°C for 886 days. The results of the tests are compared with British data[27] on the corrosion of zirconium and Zircaloy-2 in a dry CO_2 atmosphere in Table VII-4.

Table VII-3 CORROSION OF ZIRCONIUM AND ZIRCALOY-2 IN A 50 VOL.% He – 50 VOL.% CO_2 GAS MIXTURE*

	Temp., °C	Extrapolated weight gain, mg/cm^2 in 3 yr	Extrapolated weight gain, mg/cm^2 in 10 yr	Extrapolated penetration, 10^{-3} in. in 3 yr	Extrapolated penetration, 10^{-3} in. in 10 yr
Zirconium	400	2.5	5.35	0.43	0.93
Zircaloy-2	400	5.8	10.0	1.0	1.73
Zirconium	500	9.4	20.0	1.56	3.5
Zircaloy-2	500	32.5	89.0	5.5	15.3

* Data taken from reference 26.

Table VII-4 CORROSION OF ZIRCONIUM AND ZIRCALOY-2 IN DRY CARBON DIOXIDE AT 120 PSIA*

Material	Temp., °C	Extrapolated weight gain, mg/cm^2 in 1 yr	Extrapolated weight gain, mg/cm^2 in 3 yr	Extrapolated penetration, 10^{-3} in. in 1 yr	Extrapolated penetration, 10^{-3} in. in 3 yr
Iodide Zr	400	0.29	0.48	0.05	0.085
C-melted Zr	400	0.33	0.56	0.06	0.097
Arc-melted Zr 1	400	0.50	0.96	0.087	0.17
Arc-melted Zr 2	400	0.41	0.66	0.071	0.11[illegible]
C-melted Zircaloy-2	400	0.52	0.8	0.090	0.14
Iodide Zr	500	11.0	31.0	1.91	5.4
C-melted Zr	500	33.0	120.0	5.75	21.0
Arc-melted Zr 1	500	27.0	140.0	4.7	24.4
Arc-melted Zr 2	500	23.0	100.0	4.0	17.4
C-melted Zircaloy-2	500	130.0	450.0	22.6	78.0

* Data taken from reference 27.

Comparison of the two tables shows that a much lower corrosion rate at 500°C was obtained by the Hanford tests. Because of the differences in the test conditions, the reason for the lower corrosion rate is not apparent. Hanford indicates that the decrease was primarily due to a delay in the inception of breakaway corrosion caused either by the irradiation or some constituent in the gas mixture; impurities of N_2, H_2, CO, A, and O_2, in the gas mixture were said to sometimes exceed 1 per cent.

Miscellaneous Components

The Radiation Effects Information Center, Battelle Memorial Institute, recently released information on the effects of nuclear radiation on various electronic components, gaskets, glass, and hydrocarbon fuels.[28–32]

References

1. J. A. Slyh, Reactor Handbook, AECD-3647, March 1955, (pp. 133-152). (Unclassified AEC report.)
2. L. M. Currie et al., The Production and Properties of Graphite for Reactors, *Proceedings of the International Conference on the Peaceful Uses of Atomic Energy, Geneva, 1955*, 8: 451-473 (1956).
3. J. Gueron et al., Production of Nuclear Graphite in France, *Proceedings of the International Conference on the Peaceful Uses of Atomic Energy, Geneva, 1955*, 8: 474-477 (1956).
4. B. Buras, Some Experiments Concerning Pile Materials, *Proceedings of the International Conference on the Peaceful Uses of Atomic Energy, Geneva, 1955*, 8: 478-486 (1956).
5. J. Coursier et al., Determination of Traces of Boron in Graphite, Uranium, and Beryllium, *Proceedings of the International Conference on the Peaceful Uses of Atomic Energy, Geneva, 1955*, 8: 487-490 (1956).
6. A. Bezjak and S. Maricic, Correction for the Instrumental Broadening of "Two-Dimensional" lk-X-Ray-Reflection in Carbon Black Crystallite-Size Measurements, *Proceedings of the International Conference on the Peaceful Uses of Atomic Energy, Geneva, 1955*, 8: 491-495 (1956).
7. K. Wirtz, Production and Neutron Absorption of Nuclear Graphite, *Proceedings of the International Conference on the Peaceful Uses of Atomic Energy, Geneva, 1955*, 8: 496-499 (1956).
8. W. K. Woods et al., Irradiation Damage to Artificial Graphite, *Proceedings of the International Conference on the Peaceful Uses of Atomic Energy, Geneva, 1955*, 7: 455-471 (1956).
9. G. H. Kinchin, The Effects of Irradiation on Graphite, *Proceedings of the International Conference on the Peaceful Uses of Atomic Energy, Geneva, 1955*, 7: 472-478 (1956).
10. V. I. Klimenkov and Yu. N. Aleksenko, Change in the Properties of Graphite when Irradiated by Neutrons, Conference of the Academy of Sciences of the USSR on the Peaceful Uses of Atomic Energy, AEC-TR-2435 (Part 1), (July 1955). (Unclassified AEC report.)
11. W. G. O'Driscoll and J. C. Bell, Graphite: Its Properties and Behaviour, *Nuclear Engineering*, 3(32): 479 (November 1958).
12. W. G. O'Driscoll and J. C. Bell, Graphite: Its Properties and Behaviour, Part II, *Nuclear Engineering*, 3(33): 533 (December 1958).
13.* A. Legendre, J. Gueron, and H. Hering, General Study of the Nuclear Graphites Produced in France, A/CONF.15/P/1168.
14. Proceedings of the French-American Conference on Graphite Reactors, BNL-489, Nov. 12-15, 1957. (Unclassified AEC report.)
15.* A. R. Anderson et al., Chemical Studies of Carbon Dioxide and Graphite under Reactor Conditions, A/CONF.15/P/303.
16.* J. M. Blocher, Jr., and I. E. Campbell, Carbide Coatings for Graphite, A/CONF.15/P/1428.
17. J. M. Blocher et al., Niobium Carbide Coating of Graphite Tubes, BMI-1296, Oct. 6, 1958. (Unclassified AEC report.)
18. N. S. Rason and J. D. McClelland, Thermal Properties of Materials. Part I. Properties of Graphite, Molybdenum and Tantalum to Their Destruction Temperatures, WADC-TR-56-400. Wright Air Development Center, Oct. 26, 1956.
19. S. B. Austerman, Low-temperature Irradiation and Annealing Experiments in Graphite, NAA-SR-2457, July 15, 1958. (Unclassified AEC report.)
20.* R. E. Nightingale et al., Damage Effects to Graphite Irradiated upto 1000°C, A/CONF.15/P/614.
21. *Power Reactor Technology*, 1(2): (February 1958).
22. L. D. Loch, Relation Between Internal Structure and Dimensional Stability under Irradiation of Graphites, Ceramic Information Meeting Held at Oak Ridge National Laboratory, October 1-3, 1956, TID-7530(Part 2), April 1957. (Confidential AEC report.)
23.* J. L. Dickson et al., BEPO Wigner Energy Release, A/CONF.15/P/1805.
24. Nuclear Technology Briefs, Reactor Core Materials, Progress in Zirconium Technology, prepared by Battelle Memorial Institute for the USAEC, (September 1958).
25. J. P. Pemsler, The Corrosion of Zirconium Alloys in 900°F Steam, NMI-1208, August 1958. (Unclassified AEC report.)
26. R. G. Wheeler, The Effect of Reactor Atmosphere on Zirconium and Zirconium Alloys, HW-55958, May 1958. (Unclassified AEC report.)
27. C. Tyzack, Zirconium and Its Alloys, *Nuclear Engineering*, 3: 102-114 (March 1958).
28. K. E. Hassler et al., The Effect of Nuclear Radiation on Transistors. Technical Memorandum No. 5, Radiation Effects Information Center, Battelle Memorial Institute, Nov. 30, 1958.
29. J. F. Hansen, Effect of Nuclear Radiation on Electronic Transformers and Transformer Materials, Technical Memorandum No. 7, Radiation Effects Information Center, Battelle Memorial Institute, Nov. 30, 1958.

30. N. J. Broadway and S. Palinchak, The Effect of Nuclear Radiation on Seals, Gaskets and Sealants, Technical Memorandum No. 8, Radiation Effects Information Center, Battelle Memorial Institute, Nov. 30, 1958.

31. W. C. Riley et al., The Effect of Nuclear Radiation on Glass. Technical Memorandum No. 9, Radiation Effects Information Center, Battelle Memorial Institute, Nov. 30, 1958.

32. L. J. Hillenbrand, The Effect of Nuclear Radiation on Hydrocarbon Fuels. Technical Memorandum No. 11, Radiation Effects Center, Battelle Memorial Institute, Nov. 30, 1958.

* Second United Nations International Conference on the Peaceful Uses of Atomic Energy, Geneva, September 1958. (Available from the Office of Technical Services, Dept. of Commerce, Washington 25, D. C.)

U^{236} Problem in Isotope Separation Plants

If the fuel of an enriched-uranium reactor is recycled a number of times through a diffusion plant for re-enrichment, the U^{236} content may build up to a rather high value because the rate of burnout in the reactor is low and there is no other effective sink for the U^{236} produced except the waste stream from the separation plant. The radioactivity and neutron absorption problems connected with the U^{236} (and the higher isotopes produced from it in the reactor) have been considered in reference 1, which was discussed in a previous issue of this Review.[2] Reference 3 considers the effect of the U^{236} content on the cost of re-enrichment. The reference contains theoretical curves for a typical diffusion plant which show the equilibrium concentration of U^{236} in recycled fuel as a function of reactor feed enrichment, with the degree of burn-up per reactor pass as a parameter. The U^{236} concentration curves, for burn-up in the range 20 to 60 per cent, show that for reactor feed enrichments in the range 30 to 50 per cent U^{235} the U^{236} content is comparable to the U^{235} content, and that for higher enrichments U^{236} is the principal constituent other than U^{235}. The cost increase considered is only that due to the additional separative work which is done on U^{236} in achieving the equilibrium concentration corresponding to the specified U^{235} content. This extra cost is of the order of 16 per cent for a reactor feed of 80 per cent U^{235} content, decreases with U^{235} content, and is less than 1 per cent for U^{235} contents smaller than about 10 per cent. The equilibrium U^{236} content and the additional separation costs are greatly decreased if some of the diffusion plant output is bled off for other purposes such as fueling new reactors. A diversion of 25 per cent of the output decreases the U^{236} content of 50 per cent enrichment fuel by about a factor of 5. It thus appears that the extra separation cost resulting from U^{236} is not important in low-enrichment reactors and is likely to be small even for high-enrichment reactors if there is some diversion of the diffusion plant output. These conclusions apply only if the equilibrium U^{236} content, which corresponds to the diffusion plant output of fuel having the specified U^{235} content, is tolerable. The neutron absorption and radiation problems connected with this equilibrium concentration still remain.

Isotope Build-up in Recycled Fuel

The economic operation of a reactor on the thorium cycle requires the recovery and use of the U^{233} produced during the fuel irradiation. The buildup of extraneous isotopes in recycled fuel has been discussed, for both the uranium and thorium cycles in reference 4, which was reviewed previously.[2] A recent report by St. John and Toops[5] discusses a number of factors relating to the accumulation of U^{232} in the U^{233} produced during irradiation of thorium and presents a number of details in the derivation of mathematical expressions related to the formation of U^{232}. Uranium-232 is the primary source of gamma-ray activity in recycled U^{233} and, through its daughter Th^{228}, is a contributing factor to the increased gamma-ray activity of the salvaged thorium. The decay of α-active U^{232} (74-year half-life) leads to a number of radioactive daughter products, and it is the energetic gamma radiation from these daughter products which complicates the handling and fabrication of fuels using recycled U^{233}.* Since the 1.9-year Th^{228} is one of the daughter products of U^{232}, the accumulation of this isotope, prior to chemical separation of the spent thorium fuel element, contaminates the thorium recovered in the chemical processing stages. This contamination can be decreased by processing as soon after irradiation as possible, so as to minimize the growth of Th^{228}.

Uranium-232 is formed during the irradiation of thorium by either of two schemes:

*ThC (Bi^{212}) emits a 2.2 Mev gamma ray.

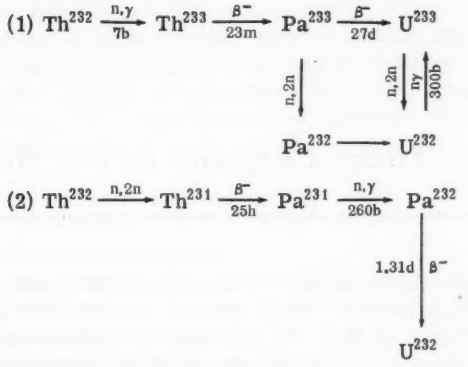

Since the cross section for the n,2n processes requires high energy neutrons and would be expected to be approximately the same for Th^{232} or U^{233}, the rate controlling step of the processes above will be the n,γ reaction on Th^{232} or Pa^{231}. The amounts of U^{232} formed by the two processes would then be in the ratio of n,γ cross sections and would therefore be predominately (~97 per cent) the second of the two schemes above. The relatively large capture cross section of U^{232} would tend to compensate for the U^{232} production in the first scheme, i.e., the n,2n reaction on U^{233}.

As sources of fast neutrons for the n,2n reaction reference 5 considers both the neutrons originating in the thorium lump itself (from U^{233} fission) and those originating in fuel elements at a distance. The computation of the U^{232} production by these neutrons is set up for solution by the Monte Carlo technique on an IBM-650 computer.

References

1. E. D. Arnold, Effect of Uranium Recycle on Transuranic Element Build-up, *Nuclear Science and Engineering*, 3(6): 707 (June 1958).
2. *Power Reactor Technology*, 1(4): (September 1958).
3. G. A. Garrett and S. A. Levin, The U^{236} Problem in the Combined Operation of Nuclear Power Reactors and Isotope Separation Plant, Second United Nations International Conference on the Peaceful Uses of Atomic Energy, Geneva, September 1958. A/CONF. 15/P/442. (Available from the Office of Technical Services, Washington 25, D. C.)
4. J. W. Ullmann, Heavy Element Isotopic Buildup, in Symposium on the Reprocessing of Irradiated Fuels Held at Brussels, Belgium, May 20-25, 1957, TID-7534 (Bk 3, Session V, p. 1080.) (Unclassified AEC report.)
5. D. S. St. John and E. C. Toops, Formation of U^{232} during the Irradiation of Thorium, DP-279, April 1958. (Unclassified AEC report.)

PROGRESS ON SPECIFIC REACTOR TYPES

HEAVY-WATER REACTORS: LEAKAGE DETECTION

The D_2O moderated reactor is under development in a number of countries; interest in the reactor type is prompted mainly by the high neutron economy attainable and by the possibility of achieving rather long fuel life with uranium of natural enrichment (see pp. 7 to 22.) Power reactors cooled and moderated by D_2O are under construction or active development in Canada,[1] Sweden,[2] Norway,[3] and the United States.[4,5] D_2O-moderated reactors cooled by gas[5] and by sodium[6] are under development in the United States, and a large gas-cooled D_2O-moderated reactor is reported to be under construction in Czechoslovakia.[7]

Perhaps the most important disadvantage of D_2O is its high cost, which in the United States amounts to $28 per pound. Obviously pertinent questions in the evaluation of D_2O reactors are the probable rate of loss of D_2O, the rate of contamination of D_2O by H_2O, and the cost of re-enriching contaminated D_2O. Babcock[4] has stated that over a two-year period the D_2O losses from the Savannah River production reactors have averaged about 3 per cent per year. He has also estimated that an average entry rate of about 2 lb per day of H_2O into the D_2O might be expected in a large power reactor. As a means of estimating the cost of removing the leakage H_2O from the D_2O, he cites the information that 1000 lb per hour of steam used to heat the calandria of a well-designed vacuum distilling tower will remove 1 lb of H_2O per day from a 99.75 per cent D_2O liquid as a 75 per cent D–25 per cent H mixture. If heat from the steam is assumed to cost 30 cents per million Btu, then the heat cost for removing H_2O would be about $8.20 per pound. Each pound of removed H_2O would be accompanied by 3 lb of D_2O; the 75 per cent D_2O-H_2O mixture would be sent to a central D_2O plant for re-enrichment at a cost of perhaps $3 to $4 per pound of contained D_2O, or $9 to $12 per pound of H_2O. Thus the operating cost for H_2O removal would amount to about $20 per pound of H_2O. To this must be added capital charges against the cost of the distilling tower. On this basis, it would appear that for reactors equipped with their own distilling towers the cost of H_2O inleakage, per pound of leakage, is comparable to the cost of D_2O outleakage.

The foregoing estimates, of course, were made for reactors cooled and moderated by D_2O. The leakage rates which characterize specific plants will depend entirely on the plant designs. A number of reactor designers hope to make considerable improvements over the estimates. For reactors which use D_2O only as moderator, the leakage expectation should be much lower, since the moderator may be unpressurized and does not require rapid circulation, and access to the moderator is not generally required for fuel changes.

Regardless of anticipated leakage rates it is obvious that effective monitoring for both inleakage and outleakage is demanded by economic considerations.

Another area of concern related to D_2O leakage is the protection of personnel. D_2O that has been irradiated in a high neutron flux is diluted to a predictable extent by tritiated water (T_2O or DTO), tritium being formed from deuterium by neutron absorption. Listed below are the three main nuclear reactions related to tritium:

$$_1H^2 + {}_0n^1 \rightarrow {}_1H^3 + \gamma \quad [\sigma = 5.7 \times 10^{-4} \text{ barns}]$$

$$_1H^3 \xrightarrow{12.4 \text{ yr}} {}_2He^3 + {}_{-1}e^0 \quad [18 \text{ kev}]$$

$$_2He^3 + {}_0n^1 \rightarrow {}_1H^1 + {}_1H^3 \quad [\sigma = 5400 \text{ barns}]$$

Leakage of tritium gas or tritiated water vapor to the air in a personnel access area presents a significant health hazard because of the

long half-life of the beta emitting decay of tritium. Tritiated water vapor is readily absorbed by lung tissue or skin and becomes uniformly distributed throughout the body. The following are significant data concerned with the hazard:

Maximum permissible body burden:	1.3 mc (ref. 8) 10 mc (ref. 9)
Maximum permissible concentration in atmosphere:	5×10^{-6} μc/cc (ref. 8) 2×10^{-5} μc/cc (ref. 9)
Maximum permissible concentration in water:	0.2 μc/cc (ref. 9)
Effective or biological half life in body:	19 days (ref. 9)

Many types of serious leakage to the air may go unnoticed with inadequate instrumentation. These include: vapor leakage from shaft seals and gaskets; leakage through small flaws in a hot pressurized system; helium leakage (many reactor designs employ a helium blanket to pressurize the D_2O and flush off fission gases or decomposed water); D_2O removal with fuel elements and transferral to handling equipment surfaces and to cooling canal and retention basin water (and also to the air above such facilities).

In the following paragraphs various instrumentation approaches to the separate phases of the leak monitoring problem are reviewed. No attempt is made to cover all possible types or variations or to propose an integrated system.

Quantitative Analysis of Water Mixtures

Infrared spectrometry is a practical and accurate technique for quantitatively analyzing mixtures of liquids. This technique is applicable where the components of the mixture have recognizably different absorption characteristics for infrared radiation.

A study of D_2O leak-detection methods based on infrared spectrometry, by Stevens and Bayly[10] at Chalk River resulted in the development of methods for determining accurately the proportions of D_2O, H_2O, and HDO in mixed water. These liquids fortunately have characteristic and differing infrared radiation absorption properties. The work was primarily concerned with the very high and very low D_2O concentration ranges.

D_2O strongly absorbs infrared radiation of 2.94 μ wave length. HDO and H_2O do not absorb this wave length as readily. Therefore, the degree of transparency of a mixture to this wave length can be taken as an indication of the D_2O concentration. Using a single beam spectrometer, properly calibrated with known mixtures, it is possible to analyze a water mixture and derive the per cent concentration of D_2O with a fair degree of accuracy. However, by splitting the light source into two equal intensity beams of the same wave length, passing one through the sample as above while the other passes through a known reference absorber, the transmission or absorption difference may be measured. Variations in the sample beam then result in magnified variations in the difference indication. A commercial double beam spectrometer has been adapted for use in this manner. A soft glass plate is used as the reference absorber in this arrangement. In the range of D_2O concentrations from 99.5 to 99.9 per cent, and with proper control, precision of ±0.003 per cent D_2O is reported. Analysis time is approximately 7 min per sample.

A difference technique similar to that described above is used to measure the degree of dilution of H_2O by HDO and D_2O.[10] In this case the width of the H_2O absorption band centered at 3.1 μ would obscure the D_2O band at 2.94 μ. However, HDO has a usable absorption band at 4.0 μ, and, as HDO is normally the major diluent in this instance, it can be successfully used. A cell filled with natural distilled H_2O is used in the reference beam. After preparation of a calibration curve from known samples, precision of ±0.01 per cent HDO or D_2O in the 1 per cent concentration range, to ±0.003 per cent in the 0.03 per cent range, is expected. Control of cell temperature in the sampling and calibration procedures is critically necessary for accuracy.

Continuous-flow Heavy-water Analyses

An instrumentation system designed for continuous monitoring of D_2O concentration in the Chalk River establishment is also described in reference 10. This system makes use of a double beam nondispersive analyzer developed by the Perkin-Elmer Corp., under the trade name of "Tri-Non." This system uses, as its

primary sensing device, what may be called a "microphone-condenser" type of transducer. This device consists of a double-walled gas chamber in which the inner wall is flexible. The inner and outer volumes of the chamber are joined by an orifice so that rapid changes in pressure in the inner chamber will result in inward and outward flexure of the inner walls with the orifice maintaining a long-term average pressure balance between the volumes and also acting as a pneumatic filter to prevent oscillation. One plate of an electrical condenser is secured to the flexible wall, while the other plate holds a fixed position in the outer volume of the chamber. Nondispersed infrared radiation passed through transparent end windows in the gas chamber is absorbed by the gas, causing heating and expansion in proportion to the absorptivity of the selected gas for the particular wave length of radiation used. In the system discussed in the reference, a mechanical "chopping" device is used to alternately permit the radiation from a beam passing through a variable optical attenuator, and a beam passing through a sample cell, to enter the gas chamber. Preliminary matching of the attenuator absorption to the absorption of a D_2O sample of known concentration, in the sample cell, results in equal absorption by the gas cell from each beam as they are alternated. Therefore, the condenser plates remain at constant spacing and the electrical capacitance is unchanged. Now, by passing a continuous unknown sample stream through the sample cell and continuing to alternate the beams at a $6\frac{1}{2}$ counts/sec rate, the heating effect and the capacitance will vary in proportion to the difference between the beam intensities at the selected wave length of radiation. The varying capacitance is used in an electrical circuit which develops an a-c signal proportional in amplitude to the absorption difference. This signal is then used in a null balance servo system which operates to continually match the variations in sample transparency by adjusting the variable optical attenuator and also to develop an output signal proportional to the per cent of variation from the reference condition. This latter signal may be continuously recorded on a strip chart. Analyzing for absorption in the 3 μ band, for changes in D_2O concentration over the 99.5 to 99.9 per cent range, a change of 0.002 per cent is said to be readily detected. The response time is of the order of 3 sec. Unfortunately, the analyzer is very sensitive to sample temperature. Therefore, provision must be made to control the sample stream temperature to within + 0.5°C of the calibration temperature before entry into the analyzer.

Heavy-water Vapor Leakage Detection

A semiportable device for probing for the point of D_2O leakage, and for assessing the leak magnitude for D_2O vapor leakage to the air, has been devised by Stevens and Bayly and is reported in reference 10. This device also makes use of a Tri-Non analyzer as its basic sensing element. The specification for the design of the system includes the requirement for minimum sensitivity to varying quantities of H_2O vapor, CO_2, and typical hydrocarbon vapors. Successful operation is reported using D_2O vapor in the sensitive gas chamber, and a mixture of the gases to be discriminated against in the filter assembly of the reference beam attenuator circuit. The air to be analyzed is drawn into the instrument at a rate of 75 cm^3/sec through a pistol gripped probe, dust filter, and flexible hose. A meter is provided on the probe, which is calibrated in grams D_2O per day at sampling rate. The device is also equipped to generate an audible signal whose pitch varies with D_2O concentration. Response time is approximately 5 sec, and the instrument is reported to be capable of sensing from 1 part D_2O vapor in 6000 parts air to 1 part in 30 parts (approximate saturation at 25°C).

Monitoring for Tritium in the Air

Care must be taken that the presence of tritium gas or tritiated water vapor (T_2O, HTO) in the air is noted rapidly. Therefore, in installations where heavy water is subject to neutron irradiation, a tritium monitoring system in personnel areas is provided.

As the characteristic decay beta emission has low average energy (18 kev), ordinary window type beta counters are not generally suitable, due to the extreme thinness required of a window for this energy. Most devices for tritium monitoring therefore use ion chambers into which the suspected sample is directly or indirectly inserted.

One such device is briefly described in reference 11. This small, portable device, designed for simplicity and rapid response, provides for drawing in a continuous flow of air through an electrostatic chamber, where the ion current, due solely to the ionization of the air by the weak beta emission, is sensed by an electrometer tube. Current amplification is provided to yield an output sufficient to operate a sensitrol relay, which in turn sets off an alarm when full scale is reached on any one of the four ranges of the instrument, covering full-scale ionization currents from 10^{-12} to 10^{-9} amp. This device is somewhat ambiguous in operation, as it senses ionization caused by other than tritium sources. However, its rapid response to a change in tritium background level warrants its investigation for general area monitoring.

A device of interest[12] developed at the Bureau of Standards for spot sampling of air for tritiated vapor is stated to be accurate for measurement of HTO vapor concentrations as low as that providing the maximum permissible exposure on a continuing 24-hr basis (e.g., 2×10^{-5} μc/ml).[8] The device uses an ionization chamber of 250 cm^3 capacity, and a vibrating reed electrometer for current measurement. In use, the chamber is evacuated in the laboratory, carried to the area to be examined, then opened to the air. The discharge of the electrometer is timed and referred to the calibration curve from which the HTO concentration may be read directly.

Routine monitoring for tritium in the plant atmosphere, as a background control means, is also accomplished by collection of atmospheric moisture from dehumidifiers or desiccators.[8] Standard ion chamber methods are used in the laboratory to evaluate the tritium content.

In a more recently developed method,[13] tritiated water is mixed with a liquid phosphor solution. Tritium content is then measured by scintillation counting.

A semiportable continuous air sampling device which has been used extensively at the Savannah River Plant[8] for probing for a point of leakage is the Kanne Chamber.[14] This device consists of a large ion chamber, a pump to sweep air through the chamber, and the associated electronics for measuring the ion current, which after calibration indicates the tritium concentration.

Monitoring for Tritium Contamination of Surfaces

Tritium contamination of a surface is difficult to detect. The usual method of detection consists of wiping the suspected surface with filter paper, then inserting the contaminated paper into a counting chamber. It is understandable that this method cannot be considered quantitative under any conditions, because of surface roughness, porosity, and crevices that cannot be touched by the filter paper. Therefore, if a filter wipe (smear test) reveals some degree of contamination, and the part cannot be removed for chemical cleaning, it is not considered unusual to paint over the surface and thereby shield against the possibility of undetectable contamination in the area of an arrested D_2O leak.

However, Colvin[15] at Savannah River Laboratory has recently devised an open-ended ionization chamber, reported to be capable of quantitative measurement of tritium on rough or smooth surfaces removed as far as $\frac{3}{4}$ in. from the open end. The chamber is a $3\frac{1}{4}$-in.-diameter dished vessel, 1 in. deep, constructed of lucite and painted with conductive paint. A center electrode, insulated from the body, extends to within $\frac{1}{4}$ in. of the plane of the open end. The chamber is operated as a dosimeter to integrate the ionization current. It is charged to a specified voltage and then placed upon the suspected surface. After a specified time has elapsed, the chamber voltage is remeasured. The decrease in voltage is proportional to the amount of tritium present. The chamber is charged and read by use of a standard electrometer. The configuration of the electrostatic field between the center electrode and the shallow outer electrode, as stated above, extends $\frac{3}{4}$ in. beyond the end of the chamber; therefore the weak tritium betas, which have a range of only $\frac{3}{16}$ in. in standard atmosphere, can contribute to chamber ionization even though they emanate from crevices or other unevenness having a considerable depth. Using this device it is stated to be possible to measure as low as 12,000 decays per minute, with a signal-to-noise ratio of 10.

References

1.* J. N. MacKay, The Canadian NPD-2 Nuclear Power Station, A/CONF.15/P/209.

2.* I. Wivstad et al., Adam—A 75 Mw Nuclear Energy Plant for House Heating Purposes, A/CONF.15/P/136.
3.* O. Dahl et al., The Halden Boiling Heavy Water Reactor, A/CONF.15/P/559.
4.* D. F. Babcock, Heavy Water Moderated and Cooled Power Reactors, A/CONF.15/P/610.
5. J. R. Dietrich and W. H. Zinn, "Solid Fuel Reactors," Addison-Wesley Publishing Company, Inc., Reading, Mass., 1958.
6. Power Reactors, U. S. Atomic Energy Commission, Technical Information Service, May 1958.
7.* A. Shevcik, Engineering and Economic Aspects of the Construction of an Atomic Power Station in Czechoslovakia, A/CONF.15/P/2092.
8.* C. M. Patterson, Radiation Protection Considerations in a Heavy Water Moderated Reactor, A/CONF.15/P/745.
9. Maximum Permissible Amounts of Radioisotopes in the Human Body and Maximum Permissible Concentrations in Air and Water, Handbook 52, National Bureau of Standards, U. S. Department of Commerce, (1953).
10.* W. H. Stevens and J. G. Bayly, Heavy Water Monitoring by Infrared Spectrometry, A/CONF. 15/P/188.
11. B. C. Eutsler et al., Instruments for Monitoring Tritium in the Atmosphere, *Nucleonics*, 14(9): (September 1956).
12. C. A. Ziegler and A. Schwebel, Technique for Monitoring Tritiated Water Vapor in Air, *Nucleonics*, 15(1): (January 1957).
13. G. T. Okita et al., Liquid Scintillation Counting for Assay of Tritium in Urine, *Nucleonics*, 14(3): (March 1956).
14. L. L. German et al., Radiological Development Activities in the Health Physics Unit. Semi-Annual Progress Report for January to June 1954, KAPL-1268, 1954. (Unclassified AEC report.)
15. D. W. Colvin, A Simple Monitor for Tritium Contamination on Surfaces, DP-242, October 1957. (Unclassified AEC report.)

*Second United Nations International Conference on the Peaceful Uses of Atomic Energy, Geneva, September 1958. (Available from the Office of Technical Services, Dept. of Commerce, Washington 25, D. C.)

An investigation of erosion and corrosion by wet oxygenated steam, by Cataldi, Cheng, and Musick, has been reported recently in the *Transactions of the American Society of Mechanical Engineering*.[1] With specific application to Dresden[2,3] dual-cycle steam conditions, the article discusses a series of preliminary laboratory tests evaluating the resistance of various materials for turbines and related components to erosion (impact, washing, wire-drawing) and corrosion (weight loss, pitting depths, crevice and galvanic attack) in the wet, oxygenated steam. Materials tested included carbon and low-alloy steels and cast iron, austenitic and ferritic stainless steels, monel, cupronickels, leaded bronze, stellite, and Ductile Ni-Resist No. 3.

Steam from a direct-cycle or dual-cycle boiling water reactor differs from usual power plant steam in several respects: it is radioactive, it may be wet, and it contains some free hydrogen and oxygen. These characteristics are discussed in references 4 and 5, which were reviewed previously.[6] The General Electric Company, in order to gain experience with the effect of oxygen on corrosion of metals in high-temperature water-steam mixtures, undertook an experimental program with the twofold purpose of: (1) aid in the selection of materials for the turbine of the Dresden Nuclear Power Station; (2) fundamental study of the effects of temperature, pressure, oxygen, velocity, and pH on erosion and corrosion by water-steam mixtures. Dresden cycle conditions are: (1) wet reactor steam at 1015 psia (545°F); (2) turbine inlet primary steam at 869 psia (525°F) and 0.5 per cent moisture; (3) secondary steam at 415 psia (450°F).

The tests conducted are grouped under three headings, corresponding to the facilities used.

Test 1. Erosion and corrosion with wet Schenectady Plant steam: 350 psia and 430°F maximum; pH 6.8; with 0.05, 80, and 110 ppm oxygen.

Test 2. Erosion and corrosion with wet steam using desuperheated steam from 14th stage of a turbine at Mystic Station of Boston Edison Company; 43 psia and 272°F, 70 to 110 ppm O_2, pH 8.8 to 9.5.

Test 3. Pitting, crevice, and galvanic corrosion tests in water and steam in autoclaves: 1015 psia (545°F), 50 and 100 ppm O_2 (initially), pH 7.

Some of the results of the tests are given in Table X-1. For complete information on the test specimens and conditions the original article should be consulted.

The following summary and conclusions were given by the authors:

1. On the basis of this preliminary evaluation, erosion and corrosion of a turbine in a boiling water nuclear power system can be maintained within tolerable limits with proper design and the selection of special materials for critical areas. This evaluation is being supplemented by continuing laboratory tests, and by the operation of a 5000 Kw turbine directly connected to a 10,000 Kw boiling water reactor at the Vallecitos Atomic Laboratory (Atomic Power Equipment Department).

2. In wet steam with low (0.05 ppm) and high (100 ppm) oxygen, stainless steels, Monel and Stellite 6 were most resistant to "wire drawing" erosion. Ductile Ni-Resist 3, low nickel steels, and low chromium steels were better than low molybdenum and carbon steels; plain cast iron was the least resistant material tested.

3. In wet steam at pH 7 and 430°F, there was no effect of oxygen on erosion in tests with high and low oxygen concentrations, except for BTH leaded bronze. With low oxygen, BTH leaded bronze resembled low chromium steel in erosion; with high oxygen, it resembled plain cast iron.

4. In wet steam at 300-430°F, and pH 7, with low and high oxygen, stainless steel, Stellite No. 1, and Ductile Ni-Resist No. 3 were most resistant to corrosion. Monel and low-alloy steels were superior to carbon steel. BTH leaded bronze was the least resistant material tested. At lower temperatures (300-400°F) and low oxygen, the cupro nickels were comparable to the most resistant materials; at high oxygen, they very rapidly approached the extreme corrosion rate of BTH leaded bronze.

5. At 300-400°F, pH 7, increasing the oxygen level from low to high increased the corrosion rate of all materials tested except stainless steel. In the case of carbon steel, this effect of oxygen on corrosion diminished rapidly with increasing tempera-

Table X-1 CORROSION RATES IN WET STEAM
(Mils per Year)

	Test 1						Test 2		Test 3			
Loop or run	1	2	1	2	1	2	A	B				
Temperature, °F	430	430	400	400	300	300	272	272	545	545	545	545
Pressure, psia	350	350	245	245	67	67	43	43	1015	1015	1015	1015
Moisture, %	9	9	7	7	5	5	6	6	Sat.	Sat.	Sat.	Sat.
Velocity, ft/sec	30	30	30	30	45	45	90	90	Rocking Autoclave			
pH	6.8	6.8	6.8	6.8	6.8	6.8	9.5	8.8	7	7	7	7
Oxygen, ppm	0.05	110	0.05	110	0.05	110	70	110	50	100	50	100
Duration	1000 hr	1150 hr	1000 hr	1150 hr	1000 hr	1150 hr	780 hr	1150 hr	6 wk	6 wk	10 wk	10 wk
Carbon steel:												
ASTM A106, A212, A201	2.0	2.2	1.0	1.4	0.2	1.0	2.6		1.5	1.6	2.0	1.2
ASTM A27 cast								2.5	0.6	0.7	0.6	0.6
Low-alloy steel:												
2½ Ni, ½ Mo, forged	0.9	1.3	0.4	0.6	0.3	0.4		1.7	0.6	0.7	0.8	0.4
2¼ Cr, 1 Mo, (A155)	1.1	1.4	0.5	1.1	0.2	0.4		0.6	0.8*	0.8*	0.5*	0.3*
Cast iron:												
ASTM A48								1.9	2.2	3.0	2.2	1.7
Ductile Ni-Resist No. 3	0.2	0.4	0.2	0.2	<0.1	<0.1		0.7		0.1		0.1
Stainless steel:												
ASTM type 304L % Sen.	0.2	0.1	0.1	0.1	0.1	<0.1	0.9		0.2	0.2		
ASTM type 347	<0.1	0.1	Nil	Nil	Nil	Nil	Nil		0.2	0.2	0.1	0.1
ASTM type 403	0.2	0.2	0.2	0.1	0.1	<0.1			0.3	0.3	0.2	0.1
Nonferrous alloys:												
90/10 Cu-Ni			0.4	4.6	0.2	0.6	1.2					
80/20 Cu-Ni			0.3	4.4	0.1	0.6						
70/30 Cu-Ni			0.2	6.8	0.1	1.3						
Monel	0.8	0.9	0.2	0.4	0.1	<0.1	0.7					
BTH Pb bronze	3.2	14.5					2.4		4.0	3.3		
Stellite No. 1	<0.1	0.1	<0.1	<0.1	<0.1	<0.1						

*2 Cr cast steel.

ture. With the cupronickels, the effect of oxygen was much more severe at 400°F than at 300°F.

6. Corrosion rates of all the materials tested, at 300-400°F, pH 7, high and low oxygen, increased with temperature, the logarithm of the corrosion rates varying approximately linearly with the reciprocal of the absolute temperature.

7. At 430°F, pH 7, with high oxygen, there was no intergranular corrosion of sensitized types 304 and 306L stainless steel specimens in 1000 hours, nor were there any cracks around stamped crosses.

8. With low oxygen, at 300-430°F, pH 7, there was no pitting observed except with carbon steel, where the effect was minor. With high oxygen, all materials pitted especially at crevices. Stainless steel and Stellite No. 1 were most resistant. Monel, cupronickel, and BTH leaded bronze were better than low-alloy steel. Carbon steel pitted most severely of the alloys tested.

9. In autoclave tests in steam-water-oxygen mixtures (545°F, 1015 psia, 50 and 100 ppm O_2) run for 6 and 10 weeks, the rates of corrosion decreased with time. The maximum depth of pitting, however, did not increase significantly.

10. In the autoclave tests, the order of resistance, as measured by the maximum depth of pitting, was the same as for the resistance to general corrosion. There was less difference in the maximum pitting depths among the ferrous alloys tested than there was in the corresponding weight losses. This reflects the greater number of pits in the least resistant alloys.

11. There were no significant galvanic or crevice effects in the autoclave tests. Naturally-formed deposits of iron oxides were more effective in promoting pitting on all classes of steel tested than were artificial 0.002-inch crevices.

12. Cast iron and low-carbon cast steel were subject to occasional very deep pits in the autoclave tests. These may be related to inclusions and/or pin-hole porosity.

References

1. H. A. Cataldi et al., Investigation of Erosion and Corrosion of Turbine Materials in Wet Oxygenated

Steam, *Transactions of the American Society of Mechanical Engineers*, 80(7): (October 1958).

2.* V. A. Elliott et al., The Dresden Nuclear Power Station, A/CONF.15/P/2372.

3. Andrew W. Kramer, "Boiling Water Reactors," Addison-Wesley Publishing Company, Inc., Reading, Mass., 1958.

4.* J. M. Harrer et al., Performance Evaluation of Direct Cycle Boiling Water Nuclear Power Plants Based on Recent EBWR and BORAX Data, A/CONF.15/P/2379.

5.* E. Beckjord et al., Operation of a High Performance Light Water Boiling Reactor, A/CONF.15/P/1923.

6. *Power Reactor Technology*, 2(1): (December 1958).

---

*Second United Nations International Conference on the Peaceful Uses of Atomic Energy, Geneva, September 1958. (Available from the Office of Technical Services, Dept. of Commerce, Washington 25, D. C.)

LEGAL NOTICE

This document was prepared under the sponsorship of the U. S. Atomic Energy Commission. Neither the United States, nor the Commission, nor any person acting on behalf of the Commission:

A. Makes any warranty or representation, express or implied, with respect to the accuracy, completeness, or usefulness of the information contained in this document, or that the use of any information, apparatus, method, or process disclosed in this document may not infringe privately owned rights; or

B. Assumes any liabilities with respect to the use of, or for damages resulting from the use of any information, apparatus, method, or process disclosed in this document.

As used in the above, "person acting on behalf of the Commission" includes any employee or contractor of the Commission to the extent that such employee or contractor prepares, handles or distributes, or provides access to, any information pursuant to his employment or contract with the Commission.

POWER REACTOR TECHNOLOGY may be purchased ($2.00 per year, $0.55 per issue) from the Superintendent of Documents, U. S. Government Printing Office, Washington 25, D. C. The use of the coupon below will facilitate the handling of your order.

POSTAGE AND REMITTANCE: Postpaid within the United States, its Territories, Canada, Mexico, and all Central and South American countries except as hereinafter noted. Add $0.50 per year, or $0.15 per single issue, for postage to all other countries, including Argentina, Brazil, British, Dutch, and French Guiana, and British Honduras. Payment should be by check, money order, or document coupons, and MUST accompany order. Remittances from foreign countries should be made by international money order, or draft on an American bank, payable to the Superintendent of Documents, or by UNESCO book coupons.

order form

SUPERINTENDENT OF DOCUMENTS
U. S. GOVERNMENT PRINTING OFFICE
WASHINGTON 25, D. C.

Enclosed:
document coupons ☐ check ☐ money order ☐

Charge to Superintendent of Documents No. _____

Please send me a one-year subscription to

POWER REACTOR TECHNOLOGY
($2.00 a year ; $0.55 per issue.)

SUPERINTENDENT OF DOCUMENTS
U. S. GOVERNMENT PRINTING OFFICE
WASHINGTON 25, D. C.

(Print clearly)

Name _____

Street _____

City _____ Zone ____ State _____